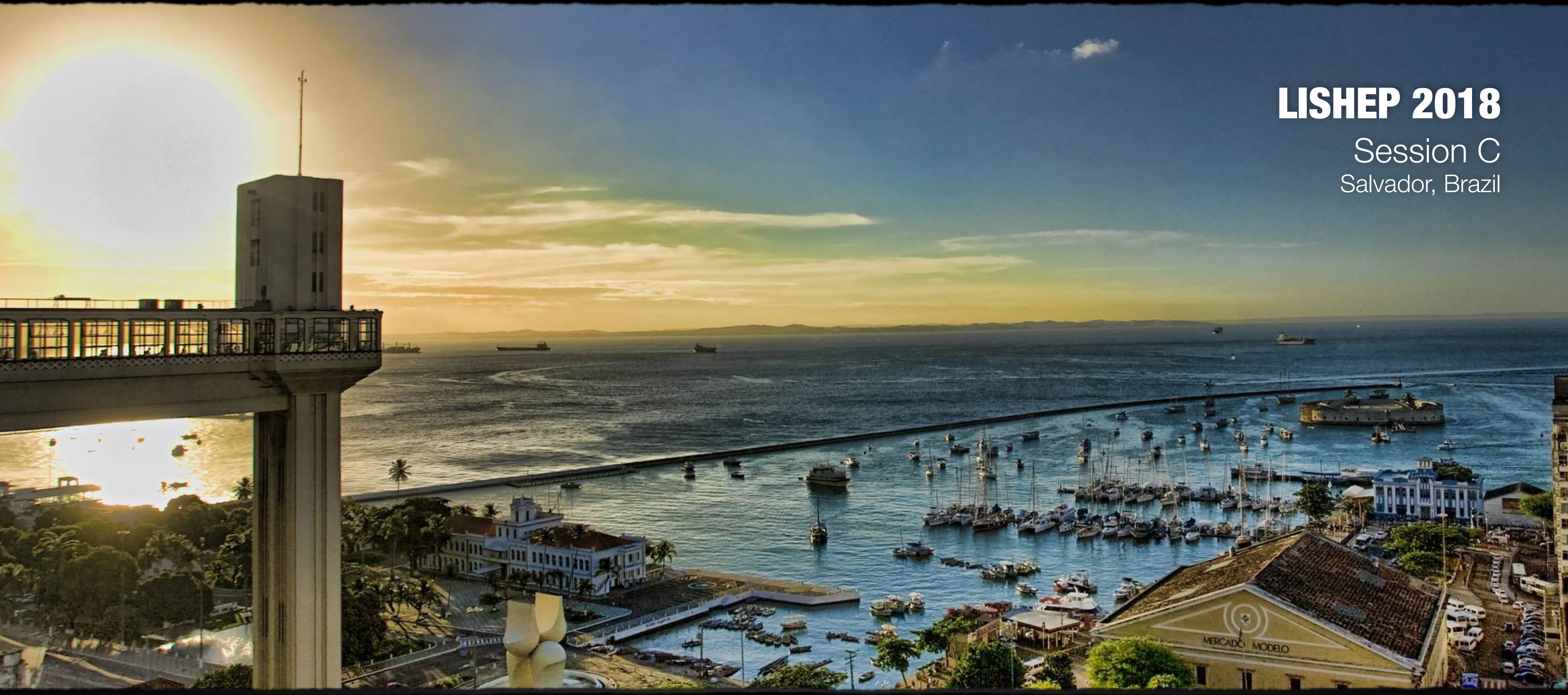

LISHEP 2018
Session C
Salvador, Brazil

FORWARD PHYSICS

Gustavo Gil da Silveira (UFRGS I UERJ)
on behalf of the CMS Collaboration

Large Hadron Collider (LHC)

The CERN—LHC complex

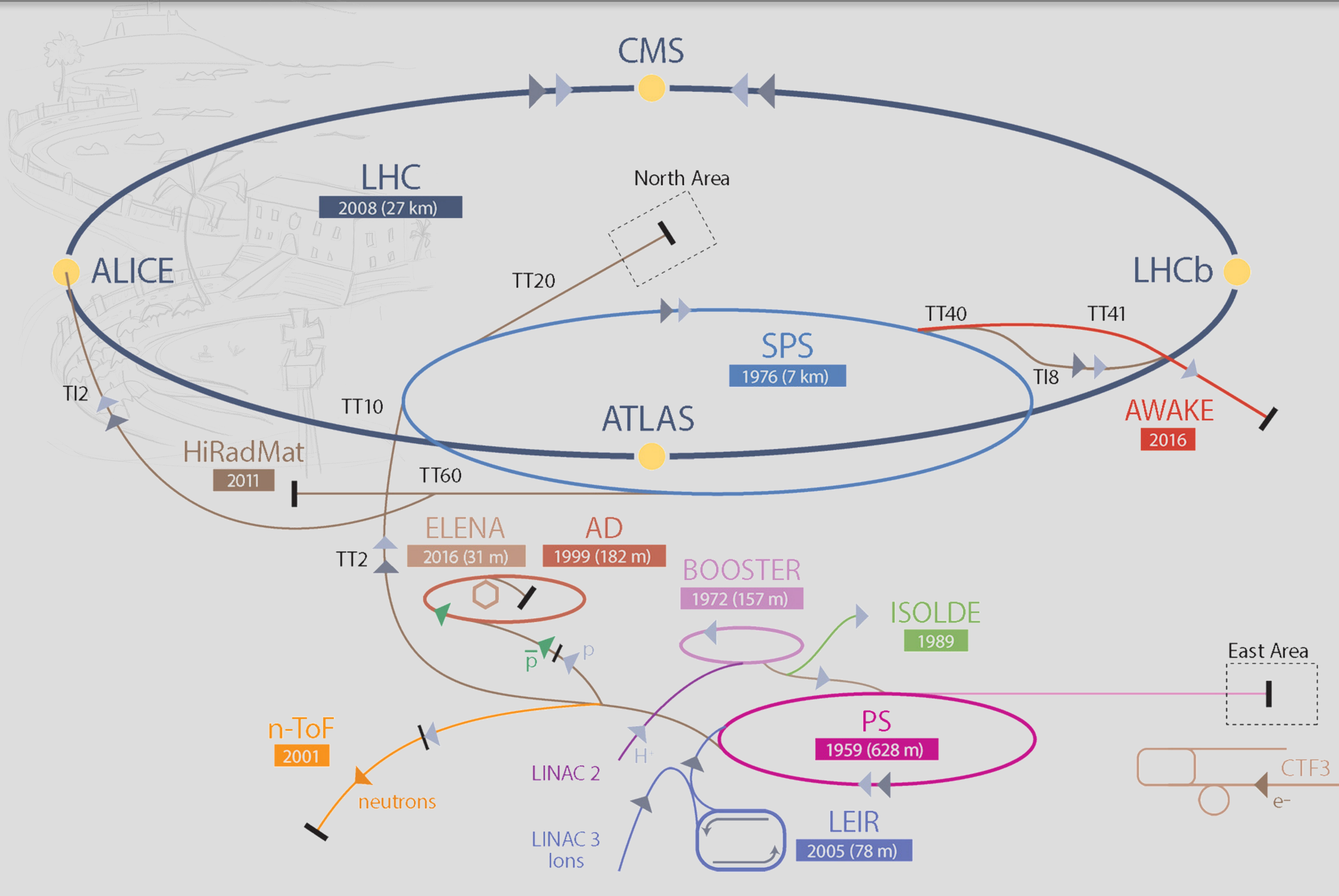

The CMS experiment

central and forward sub-detectors

Compact Muon Solenoid (CMS)

Total weight: **14 000 t**
Total diameter: **15.0 m**
Length: **28.7 m**
Magnetic field: **3.8 T**

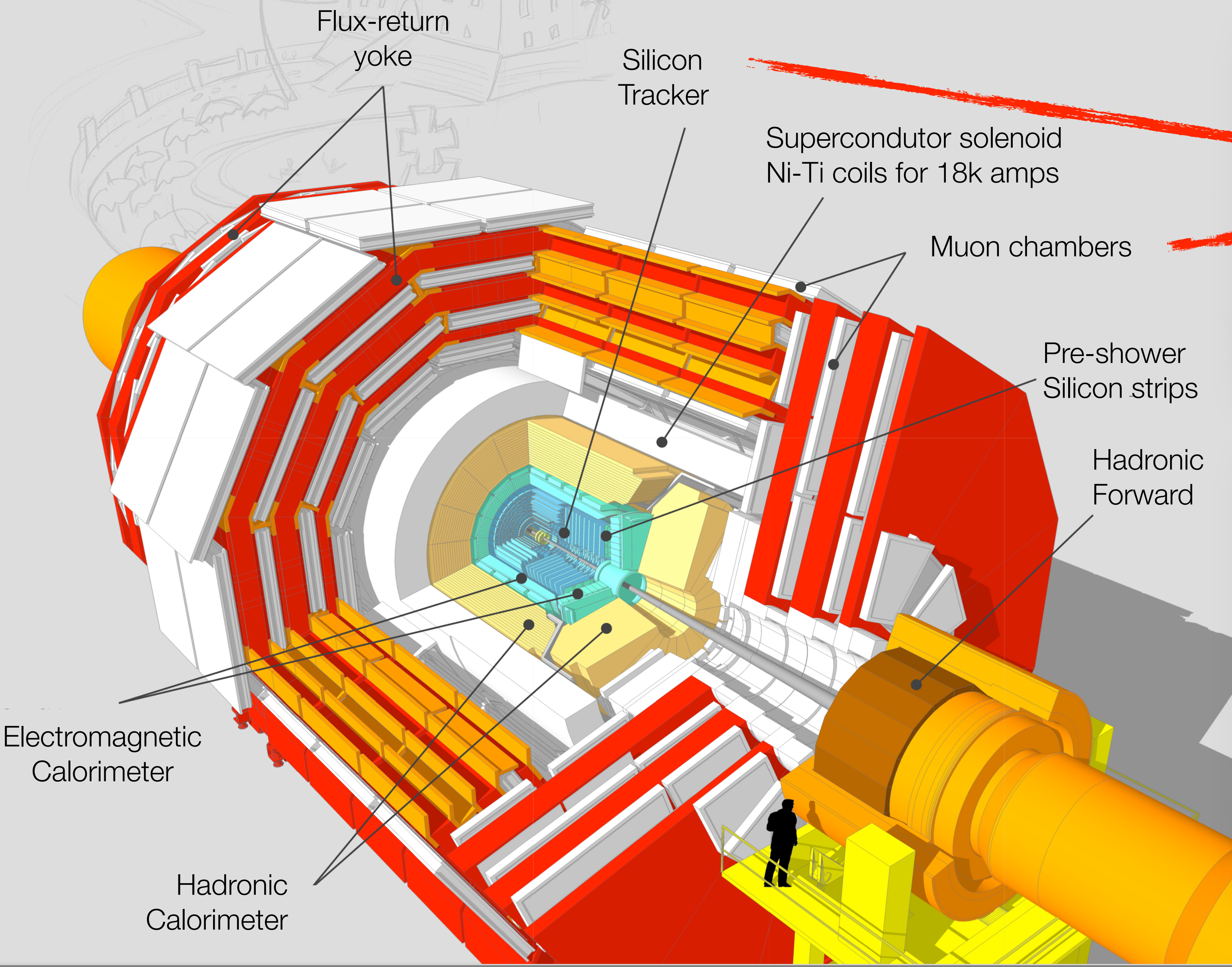

Supercondutor Solenoid

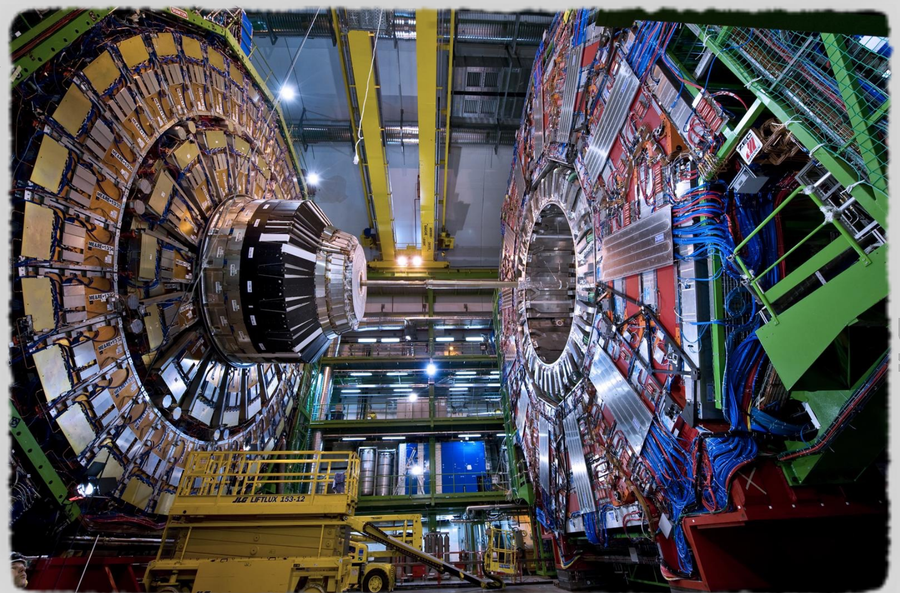

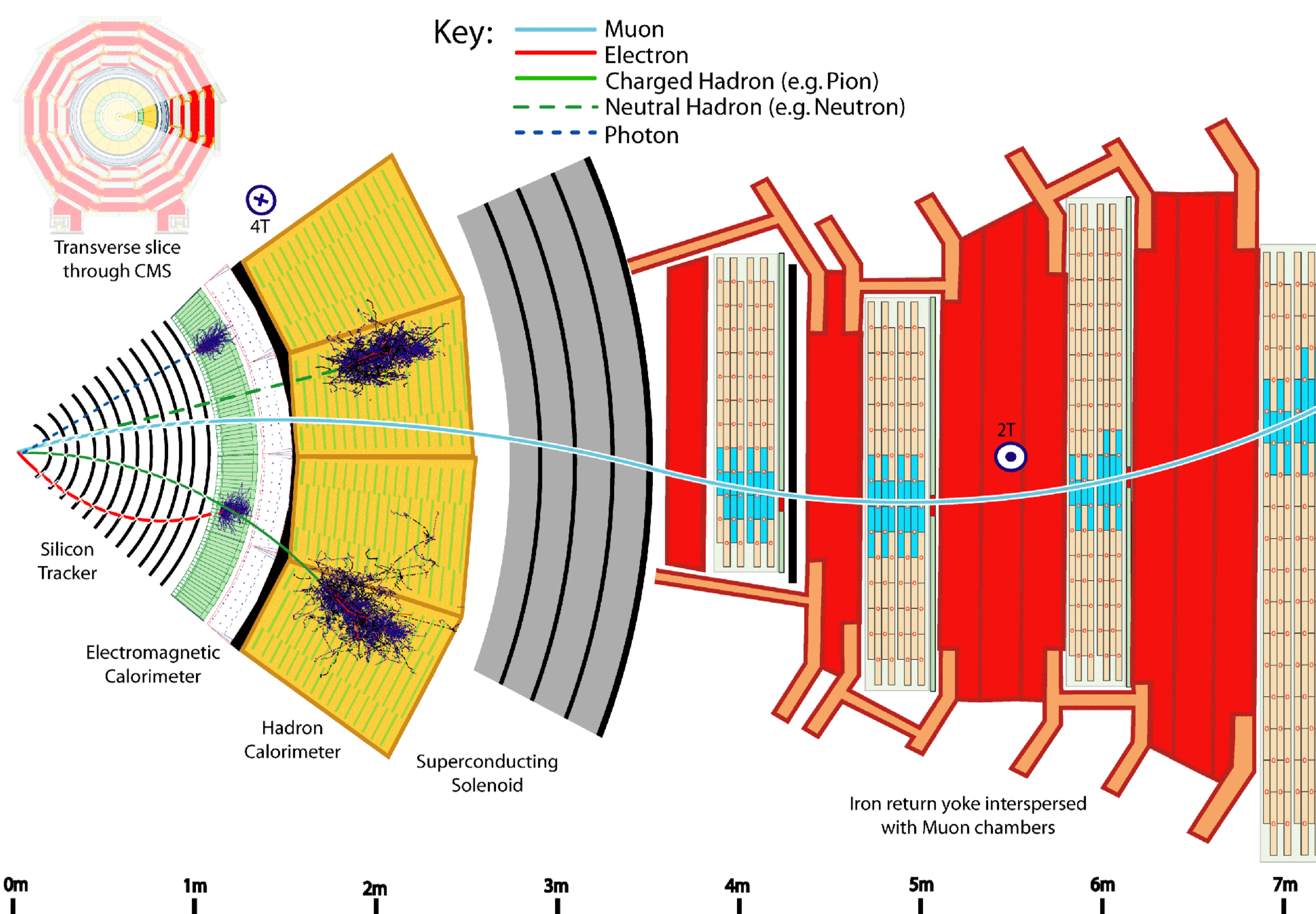

Key:
Muon
Electron
Charged Hadron (e.g. Pion)
Neutral Hadron (e.g. Neutron)
Photon
Transverse slice through CMS
4T
2T
Silicon Tracker
Electromagnetic Calorimeter
Hadron Calorimeter
Superconducting Solenoid
Iron return yoke interspersed with Muon chambers
0m
1m
2m
3m
4m
5m
6m
7m

Forward detectors

- The CMS experiment has forward sub-detectors to **enhance** its pseudorapidity coverage:

- **Hadronic Forward** (HF):

$$3.0 < |\eta| < 5.2$$

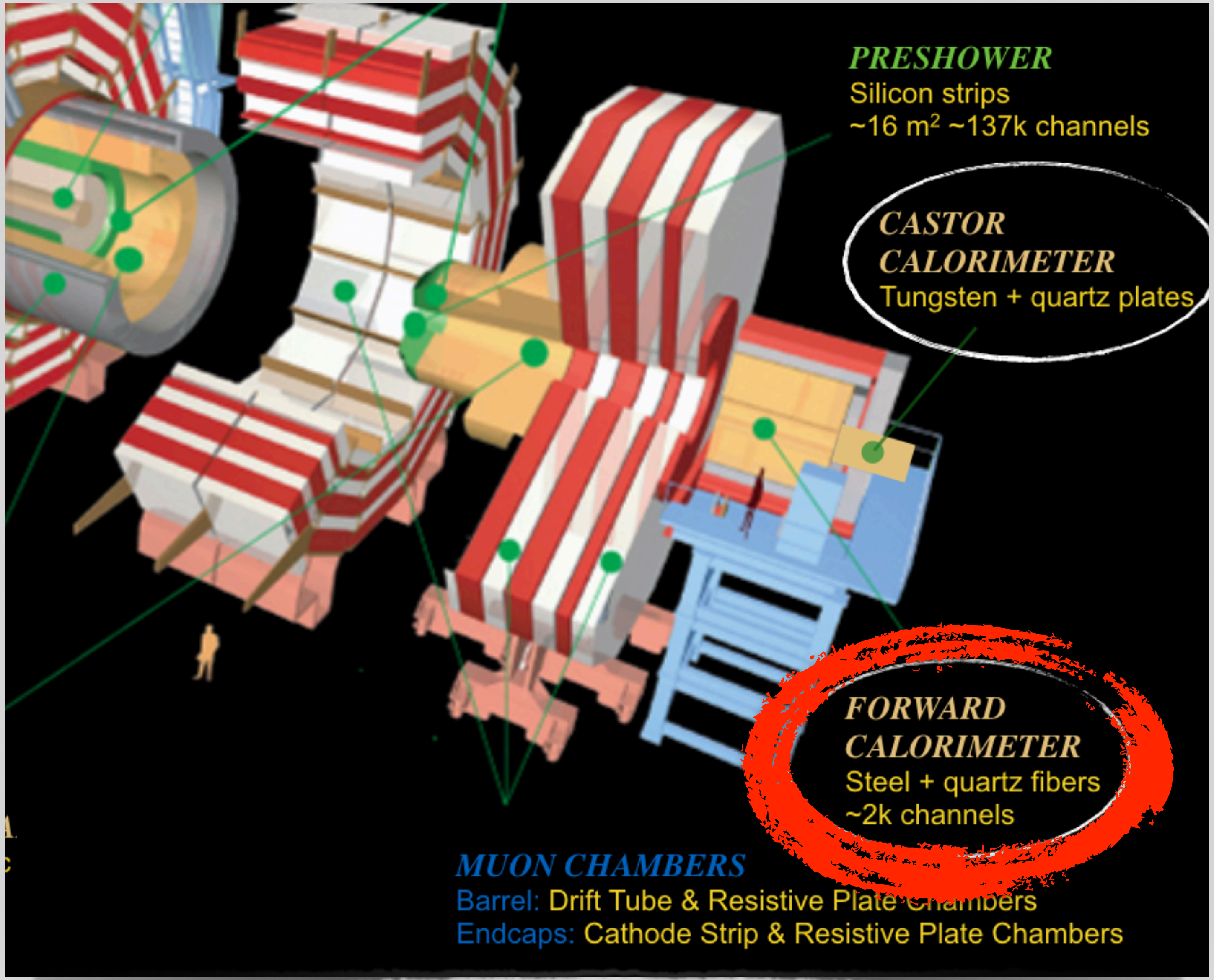

Forward detectors

- The CMS experiment has forward sub-detectors to **enhance** its pseudorapidity coverage:

- **Hadronic Forward** (HF):

$$3.0 < |\eta| < 5.2$$

  - Long and short quartz fibers (~2k channels);
  - Electromagnetic and Hadronic sections.

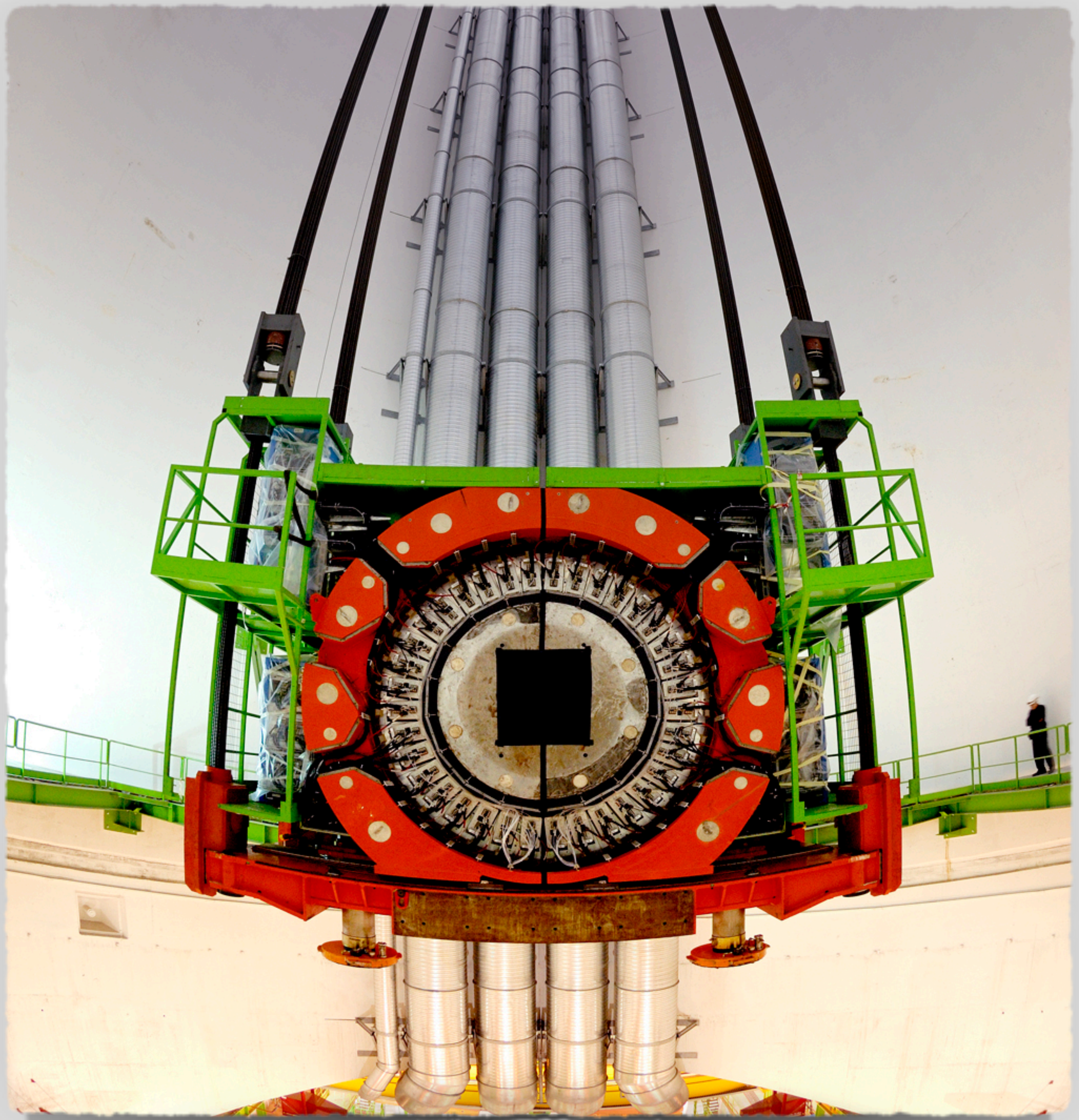

Forward detectors

- The CMS experiment has forward sub-detectors to **enhance** its pseudorapidity coverage:

- **Hadronic Forward** (HF):

$$3.0 < |\eta| < 5.2$$

- **CASTOR**:

$$-6.6 < \eta < -5.2$$

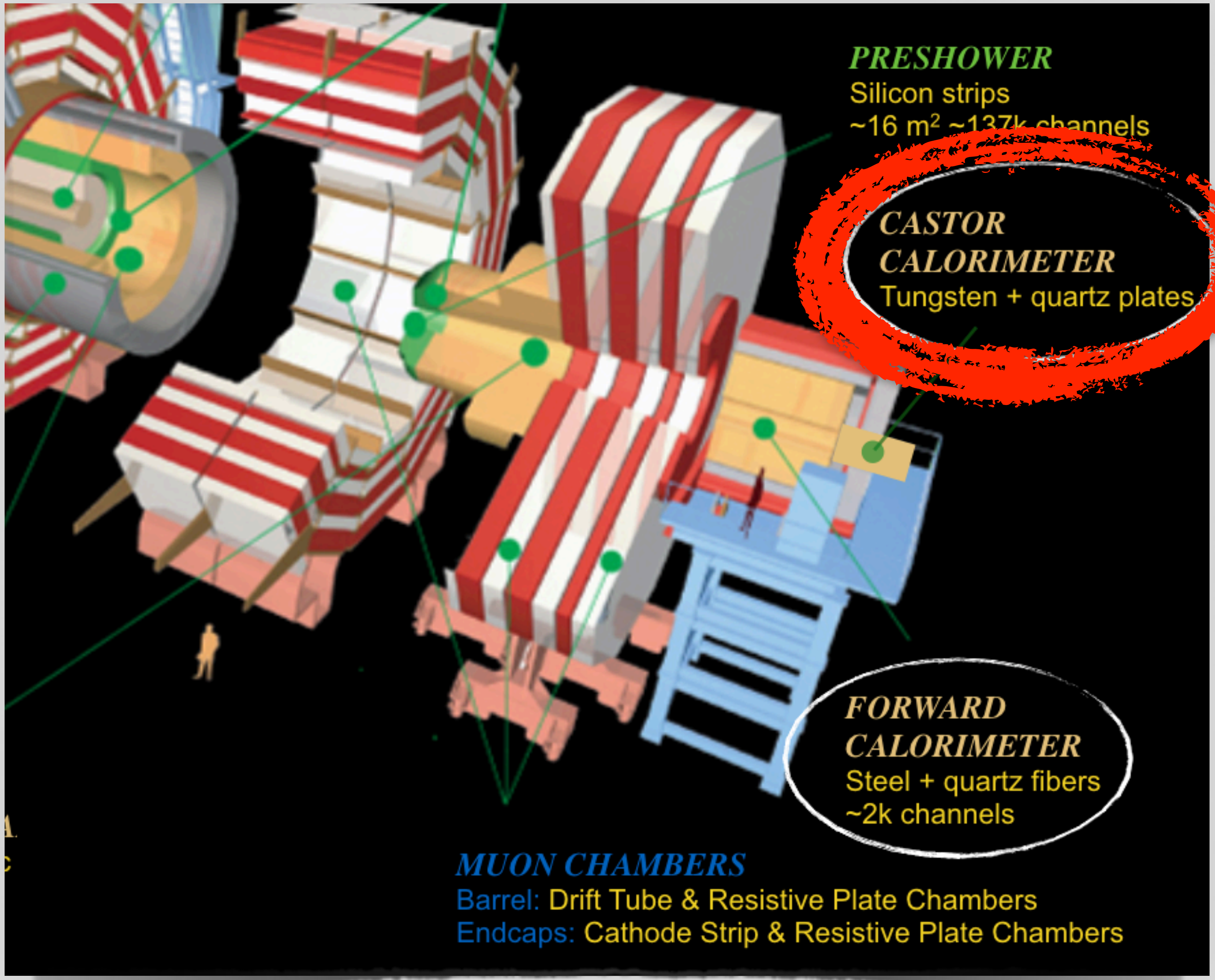

Forward detectors

- The CMS experiment has forward sub-detectors to **enhance** its pseudorapidity coverage:

- **Hadronic Forward** (HF):

$$3.0 < |\eta| < 5.2$$

- **CASTOR**:

$$-6.6 < \eta < -5.2$$

  - Tungsten and quartz plates as a sampling calorimeter;
  - Only at **minus** side of CMS;

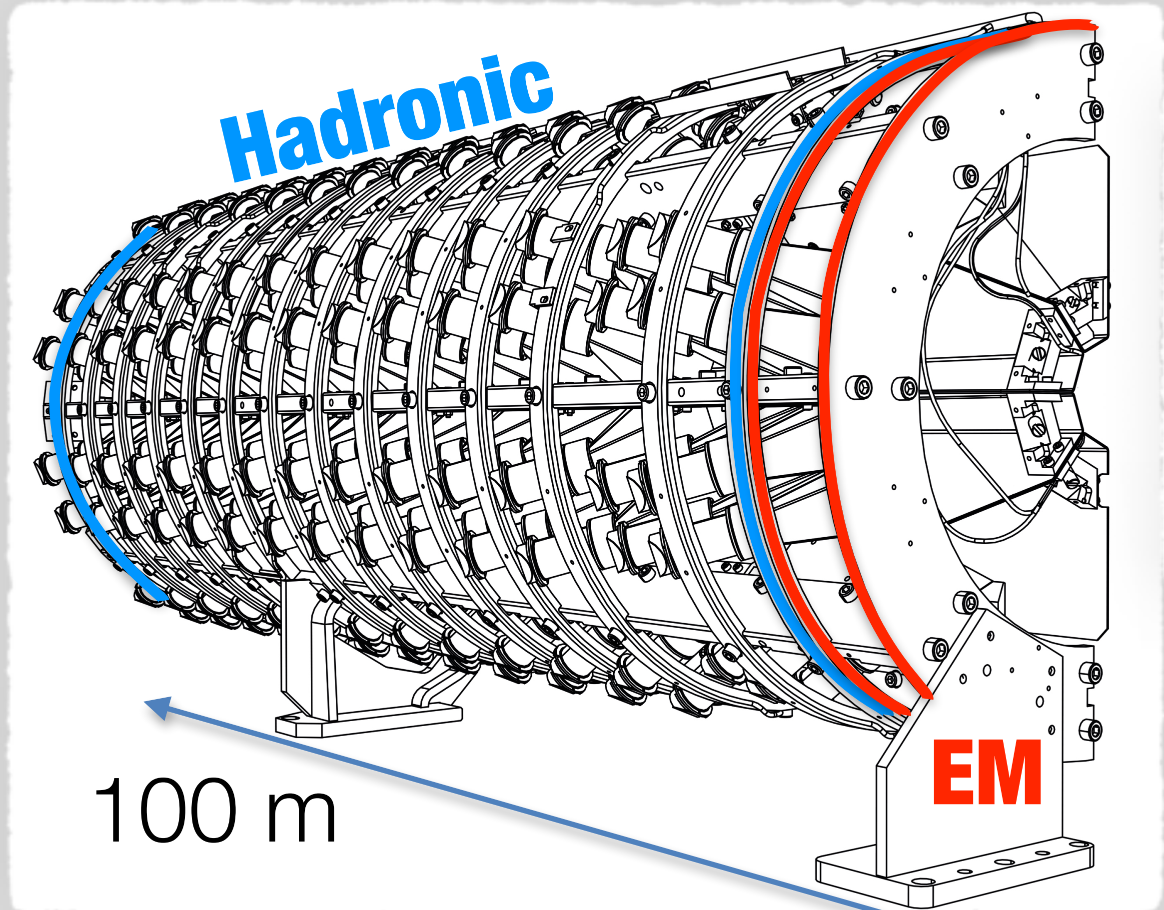

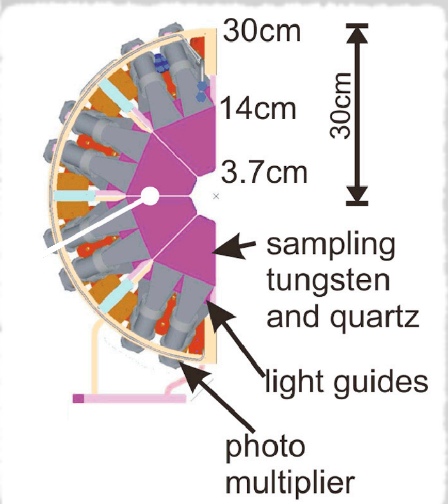

12x hadronic modules
2x EM modules

Forward Physics

Kinematical range for forward proton scattering

Phase-space region

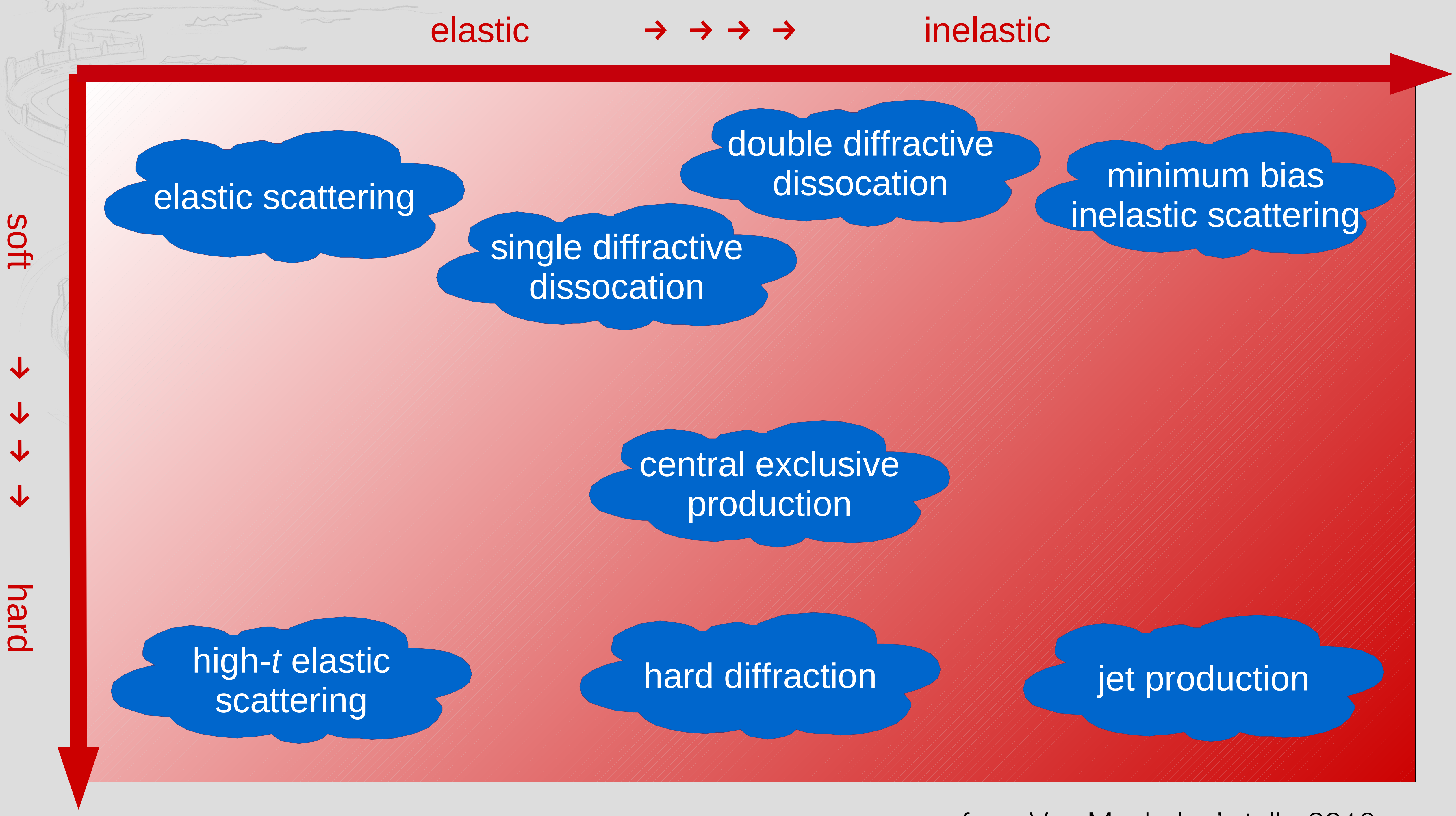

from Van Mechelen's talk, 2010

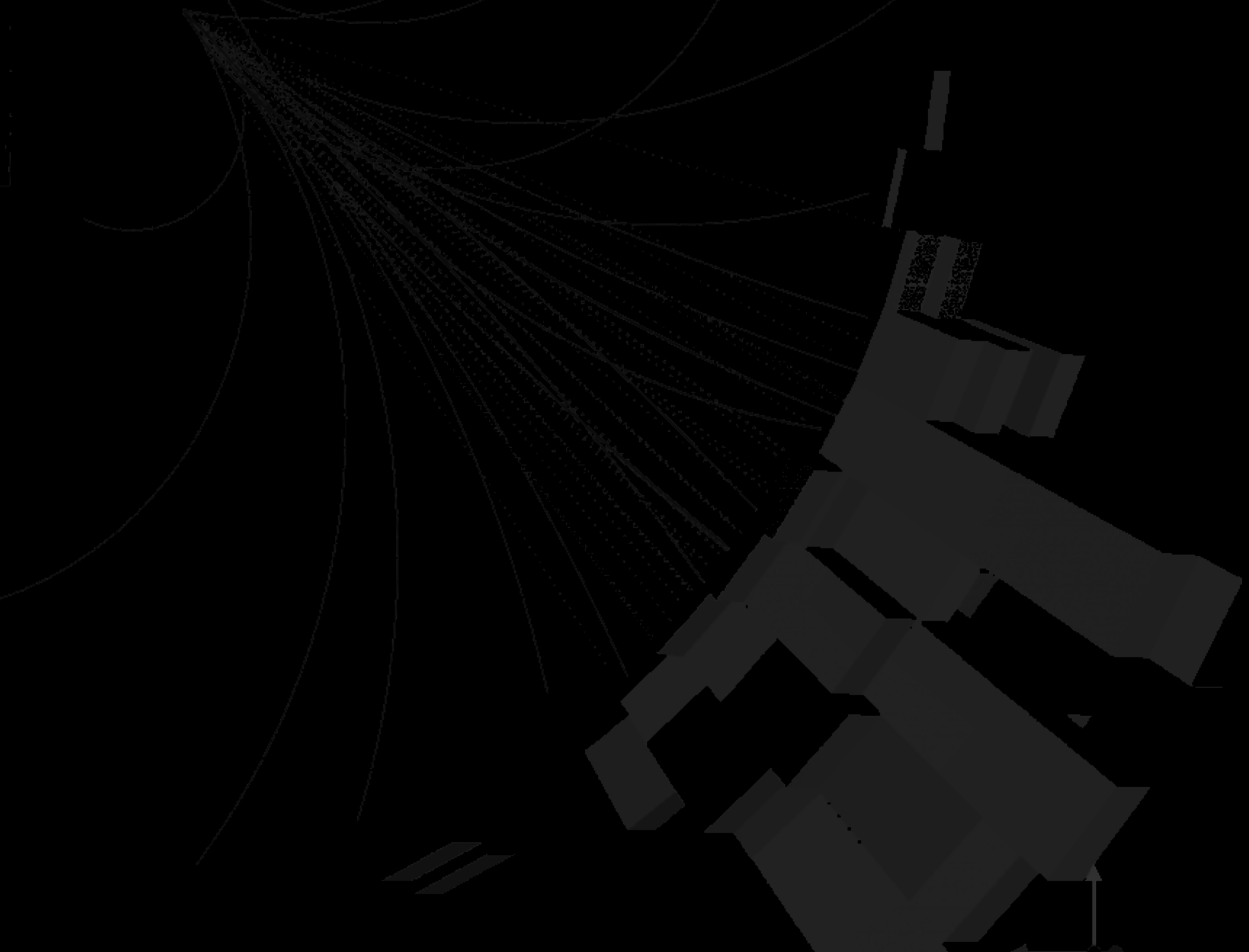

Jet-Gap-Jet

Study of dijet events with a large rapidity gap between the two leading jets in pp collisions at $\sqrt{s}$ = 7 TeV

Jet-Gap-Jet events

EPJC **78** (2018) 242
CMS-FSQ-12-001

- There is a probability to have an interaction with **large momentum transfer** to produce a pair of jets with large rapidity gap in pseudorapidity η;

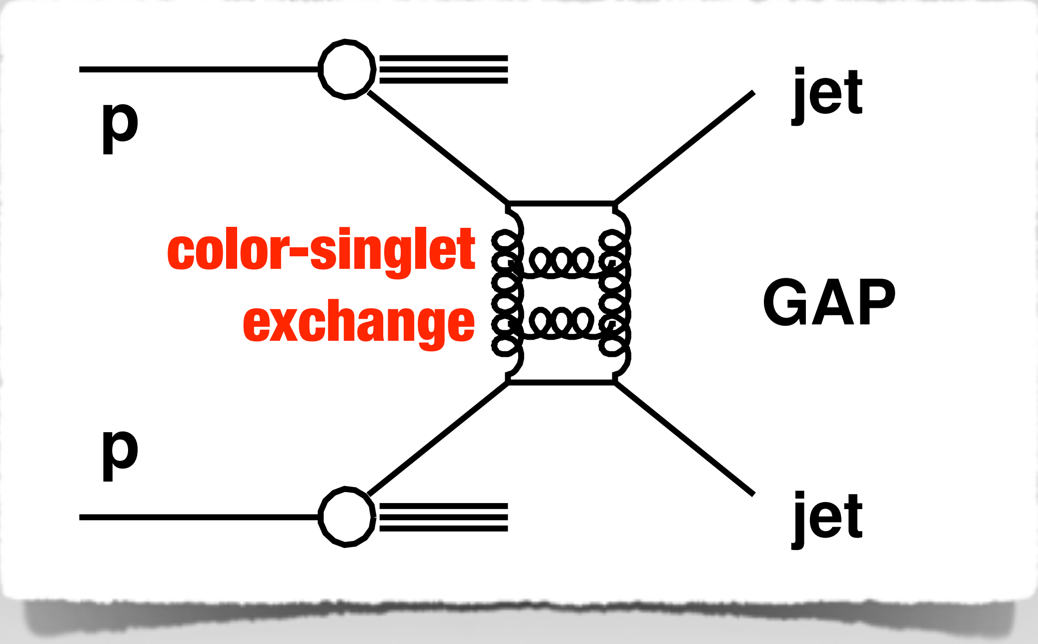

- **GAP**: no QCD radiation fills the gap, i.e., a **color-singlet exchange (CSE)** (a.k.a. diffractive event);

- Dijet production is in **general** well described by the DGLAP equation;

Jet-Gap-Jet events

EPJC **78** (2018) 242
CMS-FSQ-12-001

- There is a probability to have an interaction with **large momentum transfer** to produce a pair of jets with large rapidity gap in pseudorapidity η;

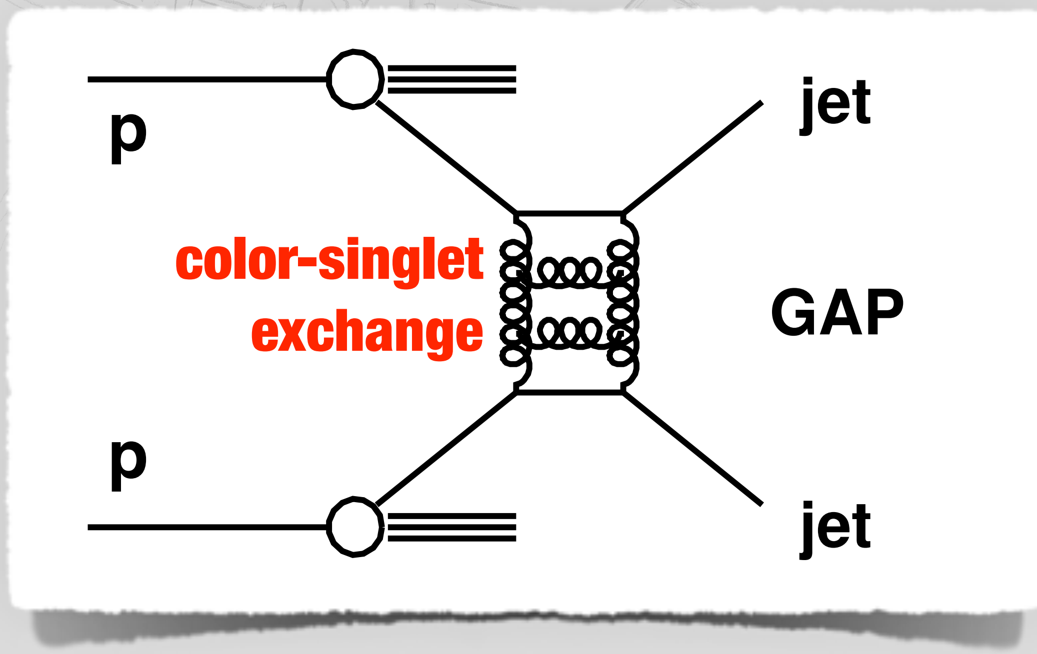

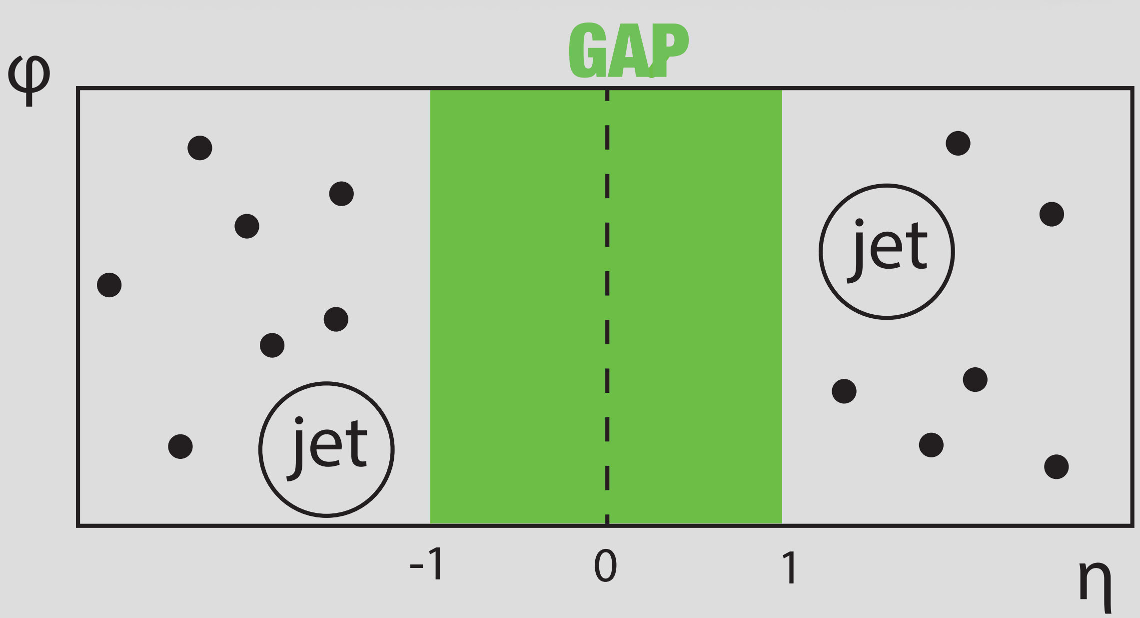

- **GAP**: no QCD radiation fills the gap, i.e., a **color-singlet exchange (CSE)** (a.k.a. diffractive event);
- Dijet production is in **general** well described by the DGLAP equation;
- The presence of a **large interval** in pseudorapidity [Δη(jj)] is better described by the BFKL equation.

LHC data

EPJC **78** (2018) 242
CMS-FSQ-12-001

- Dijet production has been seen at Tevatron and HERA;
- CMS reports the **first** observation of such event at the LHC at 7 TeV;
- The fraction of events is measured in **8/pb** of data for **2** leading jets with:

$$p_T^{\text{jet}} > 40 \text{ GeV}$$

  – reconstructed at opposite ends of CMS.

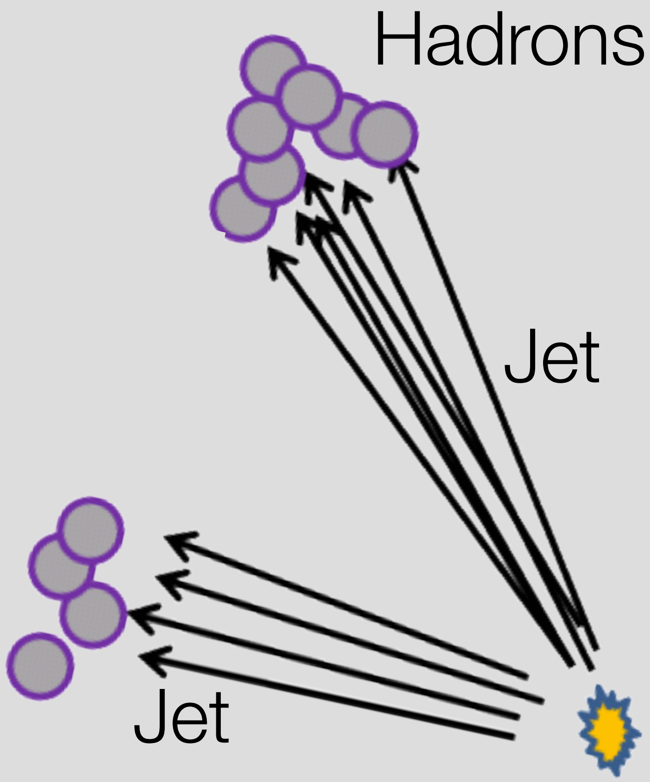

- The data are collected with **3** different triggers:
  – Threshold on uncorrected $p_T(j)$ of 15, 30, and 70 GeV.
- Single- or zero-vertex requirement rejects **most** of the events with pileup interactions.

Observables

EPJC **78** (2018) 242
CMS-FSQ-12-001

- Determine the **CSE fraction** as function of:

  1. Pseudorapidity separation in $\Delta\eta(jj)$;

  2. $p_T^{\text{jet2}}(\text{j})$ of the 2nd leading jet.

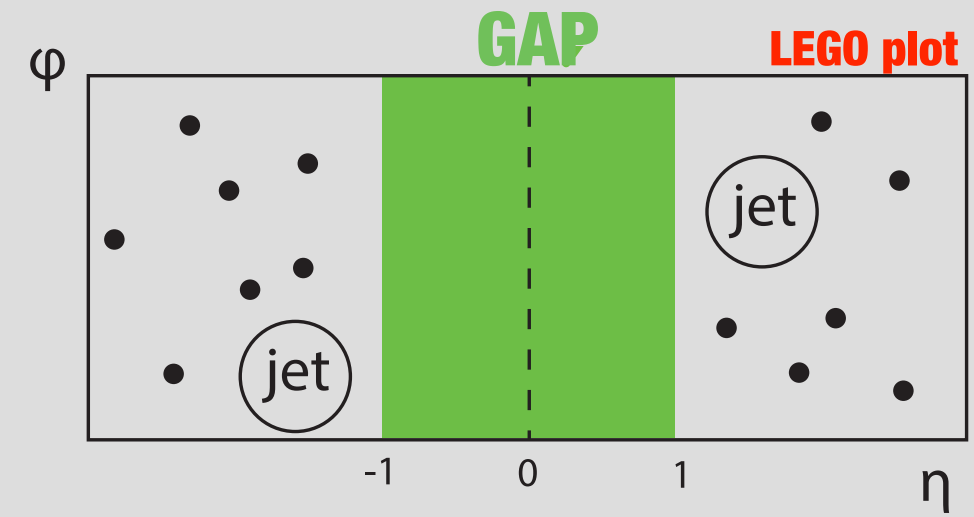

- Jets are reconstructed with infrared- and collinear-safe **anti-k_T** algorithm;

- Ranges of $p_{T,2}(\text{j})$: **40—60**, **60—100**, and **100—200** GeV;

  – Pileup corresponds to 1.16, 1.17, and 1.60.

- To ensure **pseudorapidity gaps**, additional conditions required:

  1. two leading jets with $1.5 < |\eta(\text{j})| < 4.7$;

  2. two leading jets in opposite hemispheres: $\eta(\text{j}_1)\eta(\text{j}_2) < 0$.

Observables

EPJC **78** (2018) 242
CMS-FSQ-12-001

- Determine the **CSE fraction** by:
  1. Pseudorapidity separation $\Delta\eta(jj)$;
  2. $p_T^{\text{jet2}}(j)$ of the 2nd leading jet.

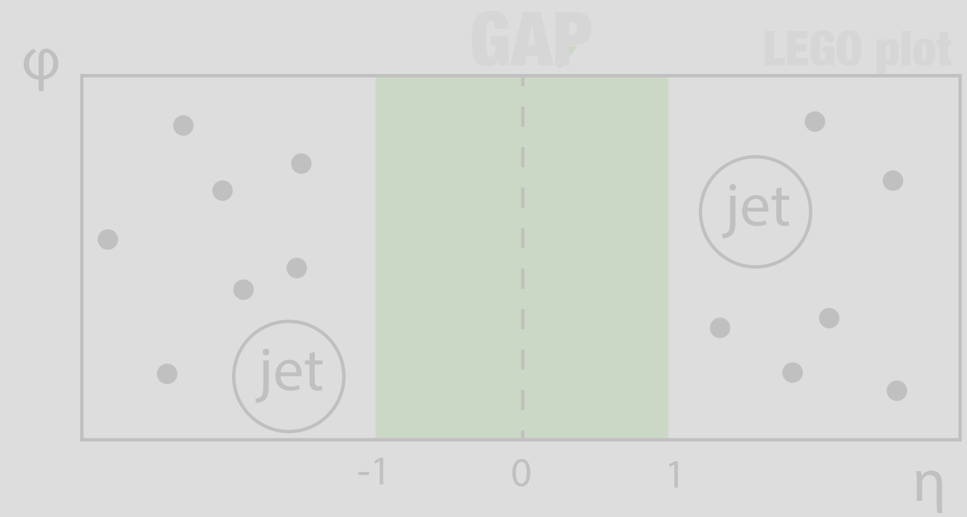

- Jets are reconstructed infrared- and collinear-safe **anti-k_T** algorithm;
- Ranges of $p_{T,2}(j)$: **40—60**, **60—100**, and **100—200** GeV;
  - Pileup corresponds to 1.16, 1.17, and 1.60 …
- To ensure **pseudorapidity gaps**, additional conditions required:
  1. two leading jets with $1.5 < |\eta(j)| < 4.7$;
  2. two leading jets in opposite hemispheres: $\eta(j_1)\eta(j_2) < 0$.

~24k events selected

N_{tracks} distribution

EPJC **78** (2018) 242
CMS-FSQ-12-001

- The N_{tracks} is obtained from a distribution of charged-particle multiplicity, N_{tracks}, with $|\eta(\text{all})| < 1$ for $p_T(\text{all}) > 0.2$ GeV, between the **2 jets**;
  - Contamination from secondary interaction **reduced** with $\frac{\sigma_{p_T}}{p_T} < 10\%$
  - Jet axes separated by **$|\Delta\eta(jj)| > 3$**, typical for diffractive studies.

N_{tracks} distribution

EPJC **78** (2018) 242
CMS-FSQ-12-001

- The N_{tracks} is obtained from a distribution of charged-particle multiplicity, N_{tracks}, with $|\eta(\text{all})| < 1$ for $p_T(\text{all}) > 0.2$ GeV, between the **2 jets**;
  - Contamination from secondary interaction **reduced** with $\frac{\sigma_{p_T}}{p_T} < 10\%$
  - Jet axes separated by **$|\Delta\eta(jj)| > 3$**, typical for diffractive studies.

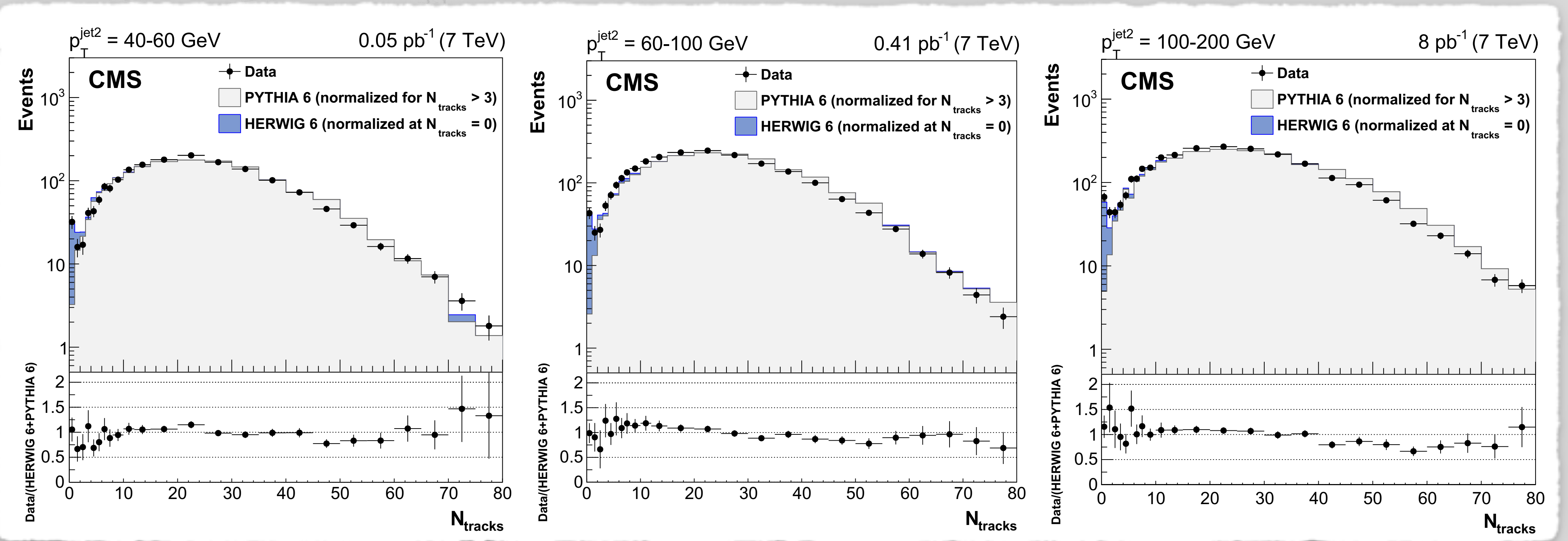

HERWIG6
CSE events

PYTHIA6
non-CSE events

Jets distributions (full p_T range)

EPJC **78** (2018) 242
CMS-FSQ-12-001

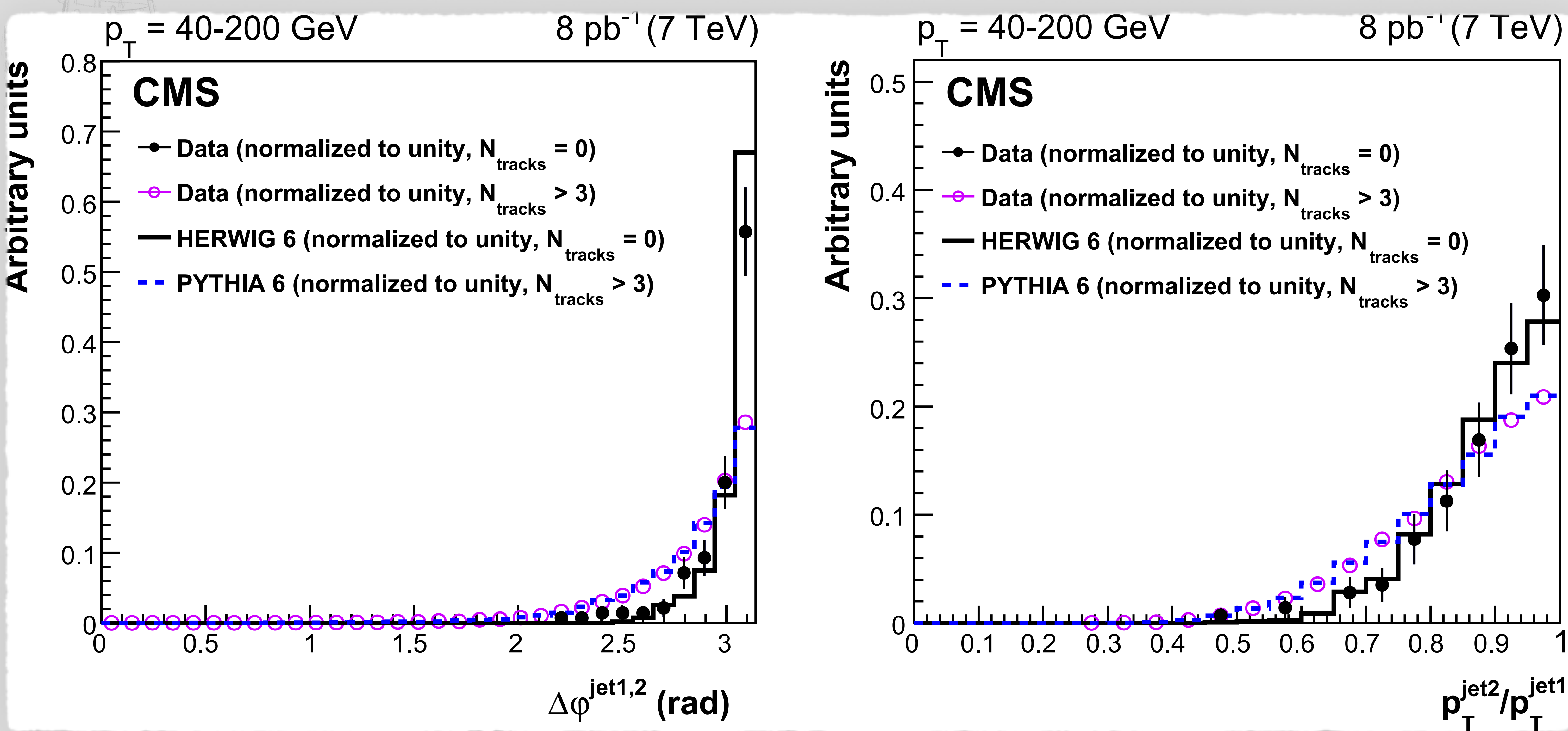

Jets distributions (full p_T range)

EPJC **78** (2018) 242
CMS-FSQ-12-001

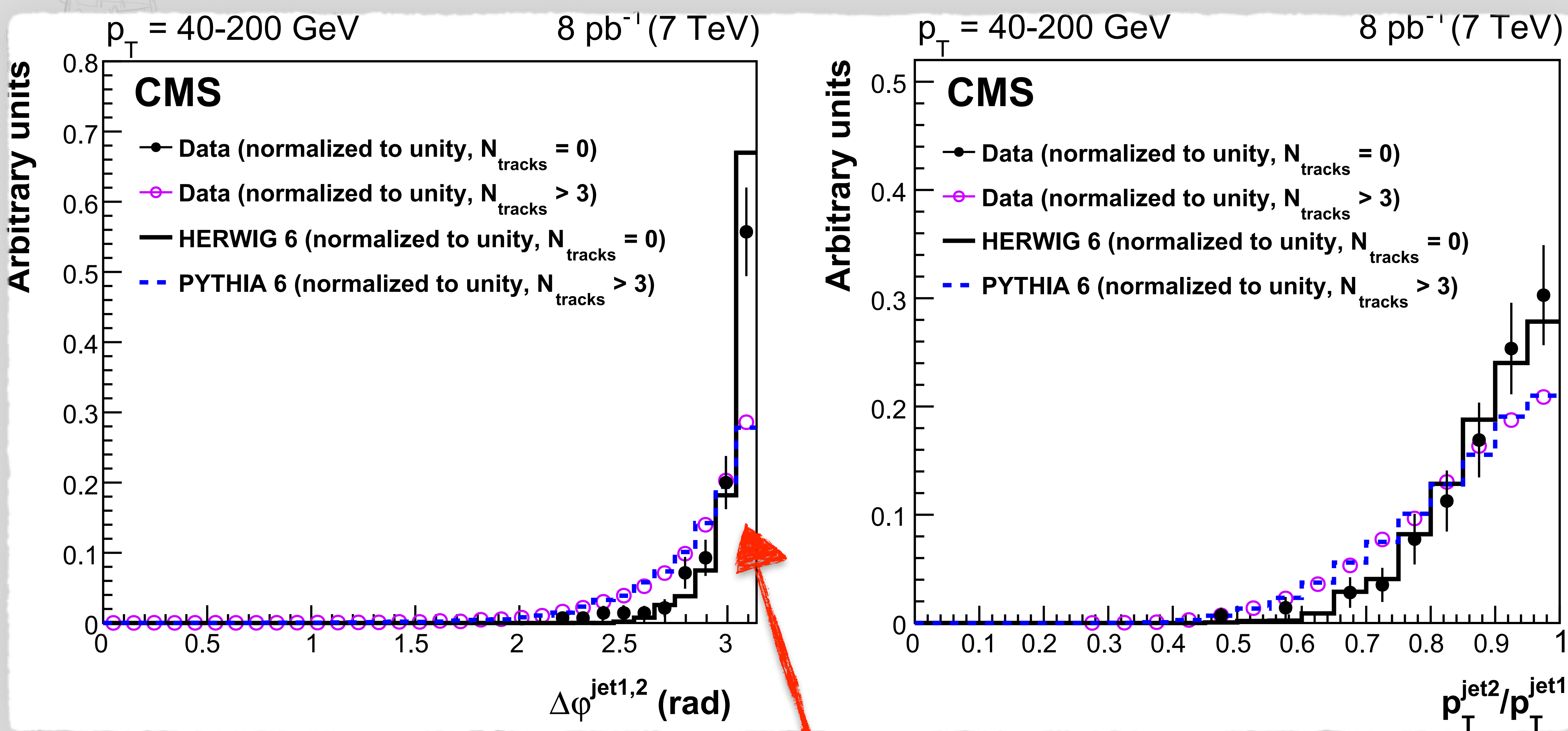

Narrow peak == clean GAP

typical for CSE events

CSE fraction (I)

EPJC **78** (2018) 242
CMS-FSQ-12-001

- The **fraction** of diffractive events is defined as:

$$f_{\mathrm{CSE}} = \frac{N^{\mathrm{F}}_{\mathrm{events}} - N^{\mathrm{F}}_{\mathrm{non\text{-}CSE}}}{N_{\mathrm{events}}}$$

$N^{\mathrm{F}}_{\mathrm{events}}$
#events in first bins of N_{tracks}

  – **Insensitive** to trigger eff. and jet reconstruction uncertainty.

- Similar selection as DØ and CDF results, with **minimal** effect of gap sizes;

$p_{\mathrm{T}}^{\mathrm{jet2}}$ range (GeV)	$\langle p_{\mathrm{T}}^{\mathrm{jet2}} \rangle$ (GeV)	f_{CSE} (%)	
40–60	46.6	$0.57 \pm 0.13 \pm 0.09$	$N_{\mathrm{tracks}} < 2$
60–100	71.2	$0.54 \pm 0.12 \pm 0.04$	$N_{\mathrm{tracks}} < 2$
100–200	120.1	$0.97 \pm 0.15 \pm 0.03$	$N_{\mathrm{tracks}} < 3$

CSE fraction (I)

EPJC **78** (2018) 242
CMS-FSQ-12-001

- The **fraction** of diffractive events is defined as:

$$f_{\mathrm{CSE}} = \frac{N^{\mathrm{F}}_{\mathrm{events}} - N^{\mathrm{F}}_{\text{non-CSE}}}{N_{\mathrm{events}}}$$

$N^{\mathrm{F}}_{\mathrm{events}}$
#events in first bins of N_{tracks}

  – **Insensitive** to trigger eff. and jet reconstruction uncertainty.

- Similar selection as DØ and CDF results, with **minimal** effect of gap sizes;

$p_{\mathrm{T}}^{\mathrm{jet2}}$ (GeV)	40–60		60–100		100–200	
$\Delta\eta_{\mathrm{jj}}$ range	$\langle\Delta\eta_{\mathrm{jj}}\rangle$	f_{CSE} (%)	$\langle\Delta\eta_{\mathrm{jj}}\rangle$	f_{CSE} (%)	$\langle\Delta\eta_{\mathrm{jj}}\rangle$	f_{CSE} (%)
3–4	3.63	$0.25 \pm 0.20 \pm 0.04$	3.62	$0.47 \pm 0.19 \pm 0.05$	3.61	$0.78 \pm 0.21 \pm 0.06$
4–5	4.46	$0.41 \pm 0.16 \pm 0.14$	4.45	$0.47 \pm 0.16 \pm 0.08$	4.41	$0.99 \pm 0.23 \pm 0.06$
5–7	5.60	$1.24 \pm 0.32 \pm 0.10$	5.49	$0.91 \pm 0.32 \pm 0.21$	5.37	$1.95 \pm 0.69 \pm 0.44$

CSE fraction increases for Δη(jj)

CSE fraction (II)

EPJC **78** (2018) 242
CMS-FSQ-12-001

- Results show that the fraction **increases** with $p_T^{\text{jet2}}(\text{j})$;
  - This confirms that the <u>diffractive</u> cross section decreases **less rapidly** than the <u>inclusive</u> cross section does.
- Fraction also **decreases** with <u>increasing</u> colliding energy;
  - More MPI results in **smaller** gap survival probability.

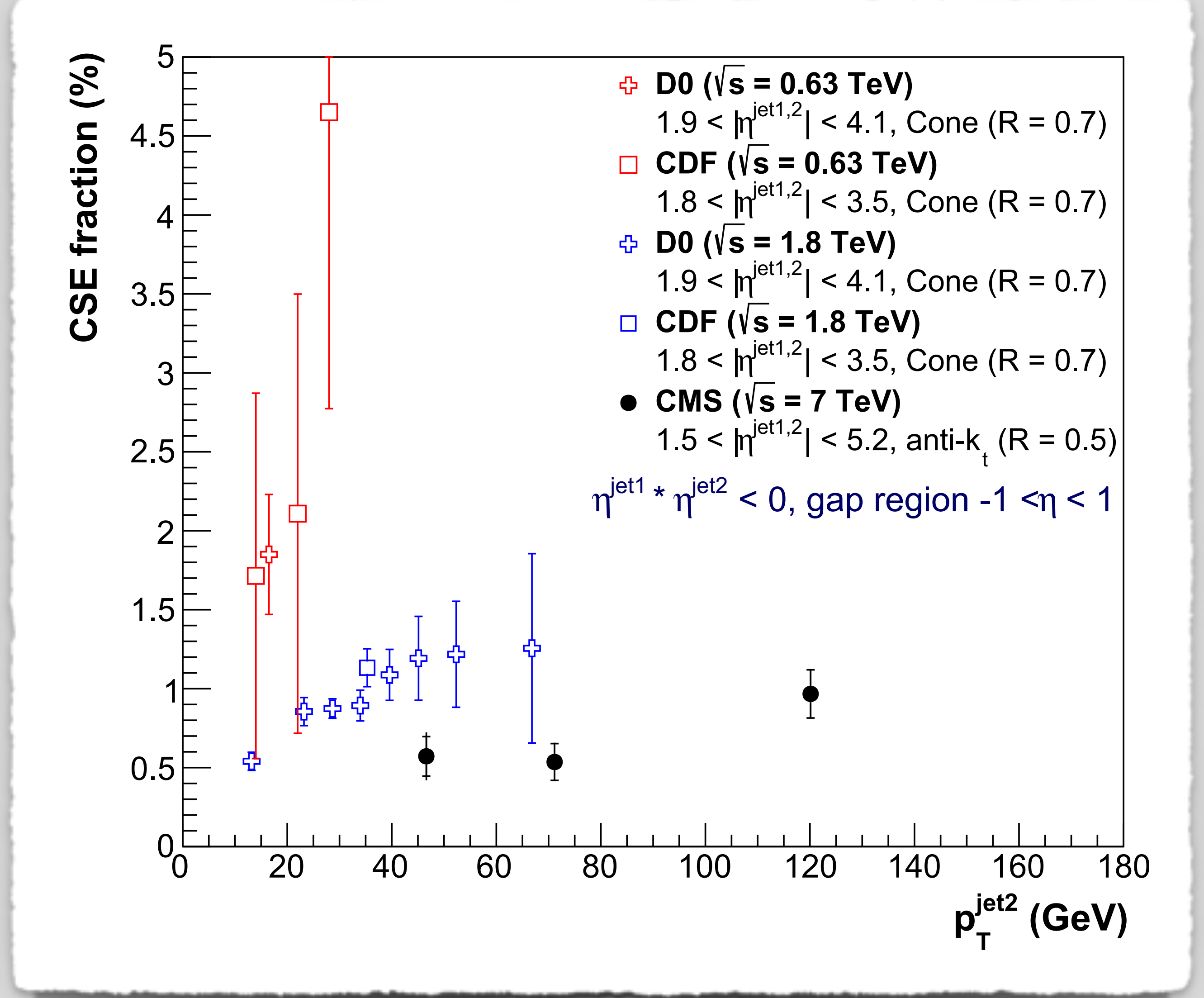

inclusive Jets

Very forward inclusive jet cross sections in p+Pb collisions at $\sqrt{s_{NN}}$ = 5.02 TeV

Gluon recombination

Public
CMS-FSQ-17-001

- Studies in proton-Nucleus collisions are suitable for searchers of signals of **gluon saturation**;
- This goal leads to the investigation of **nonlinear effects** and alternatives for the description of **parton evolution equations**;

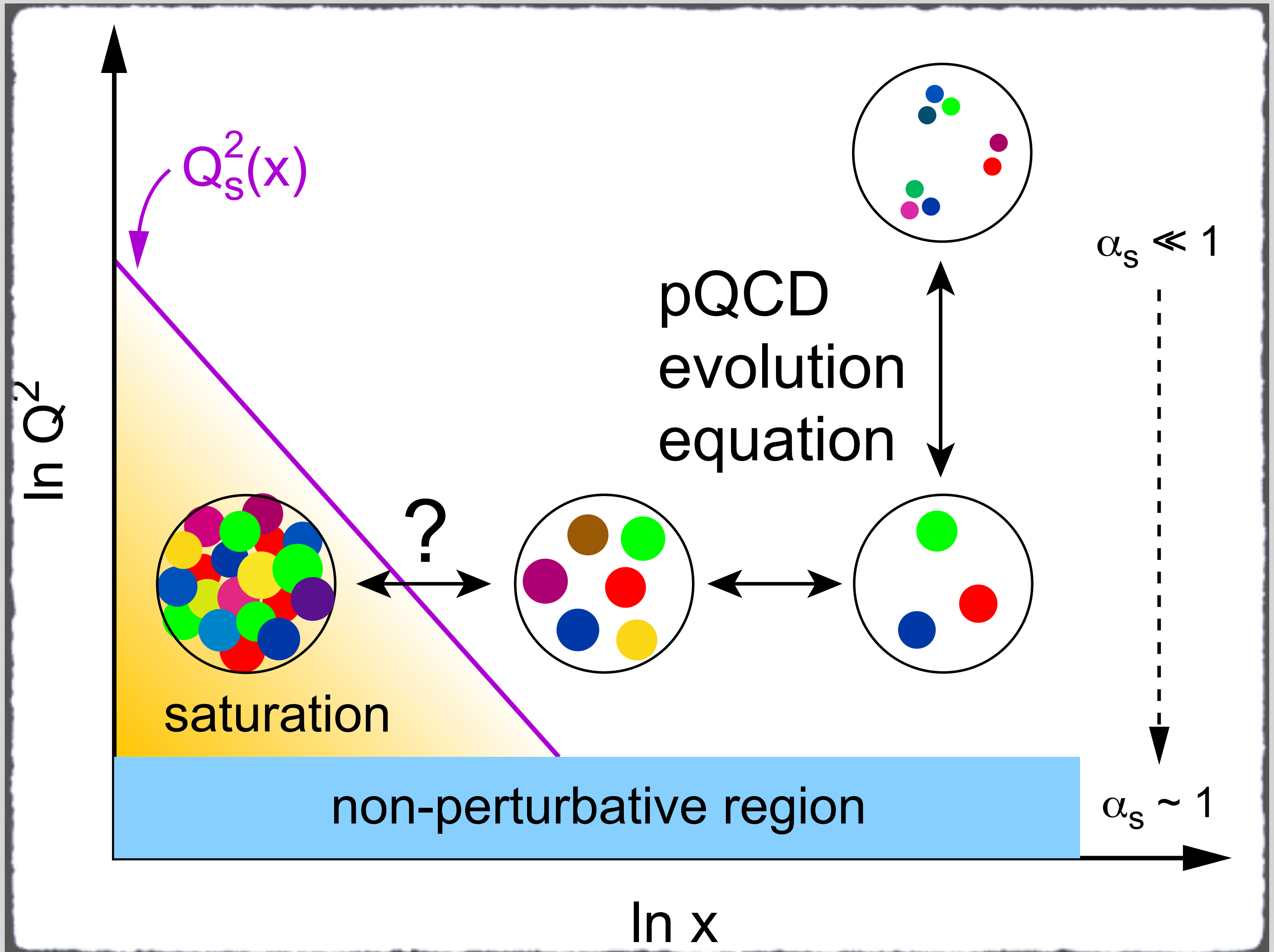

Gluon recombination

Public
CMS-FSQ-17-001

- Studies in proton-Nucleus collisions are suitable for searchers of signals of **gluon saturation**;

- This goal leads to the investigation of **nonlinear effects** and alternatives for the description of **parton evolution equations**;

- Nonlinear effects can be studied with low *x* partons by measuring **low p_T jets** in *p*-Pb collisions.

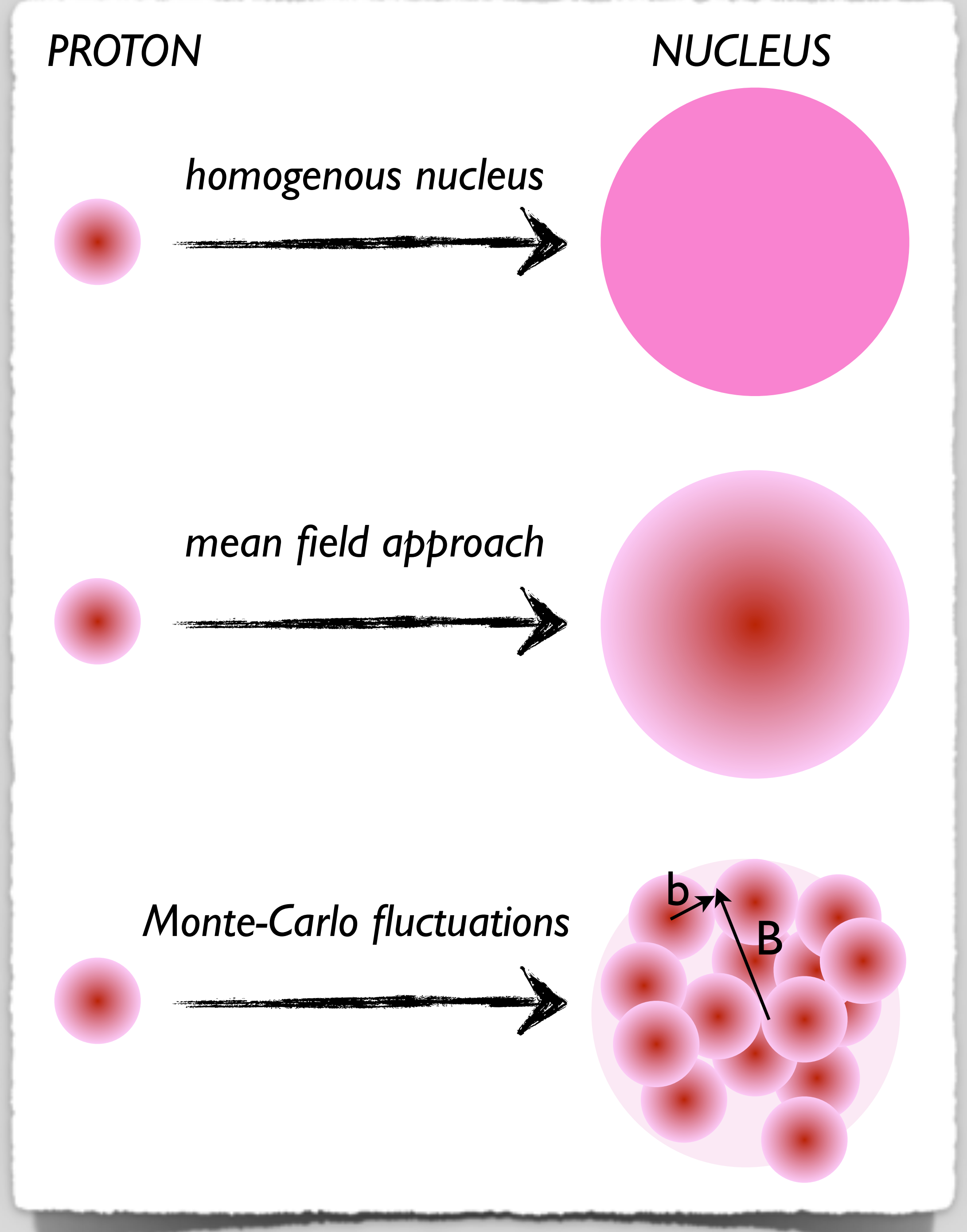

Measuring jets

Public
CMS-FSQ-17-001

- CMS makes use of **CASTOR** to measure low p_T jets at a pseudorapidity range of $-6.6 < \eta < -5.2$ in **non-diffractive events**;
  - This analysis extends previous CMS results in proton-proton collisions at **7** and **13** TeV.
- Jets selected with $\boldsymbol{p_T} \gtrsim$ **4 GeV** in p-Pb (3.13/nb) and Pb-p runs (6.71/nb);
  - Minimally **one** tower deposit above 4 GeV in HF.

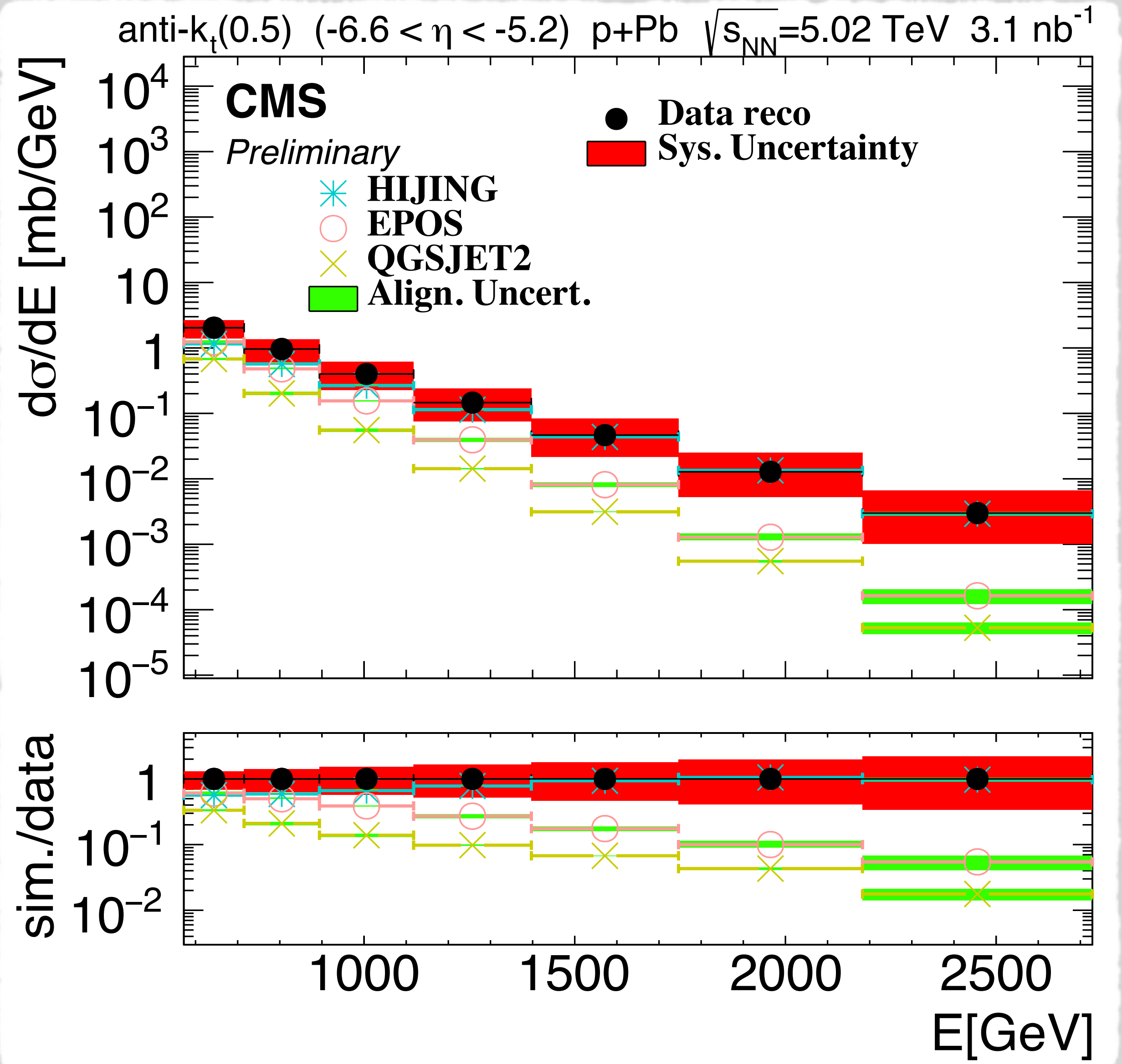

Measuring jets

Public
CMS-FSQ-17-001

- CMS makes use of **CASTOR** to measure low p_T jets at a pseudorapidity range of $-6.6 < \eta < -5.2$ in **non-diffractive events**;
  - This analysis extends previous CMS results in proton-proton collisions at **7** and **13** TeV.
- Jets selected with $\boldsymbol{p_T} \gtrsim$ **4 GeV** in p-Pb (3.13/nb) and Pb-p runs (6.71/nb);
  - Minimally **one** tower deposit above 4 GeV in HF.

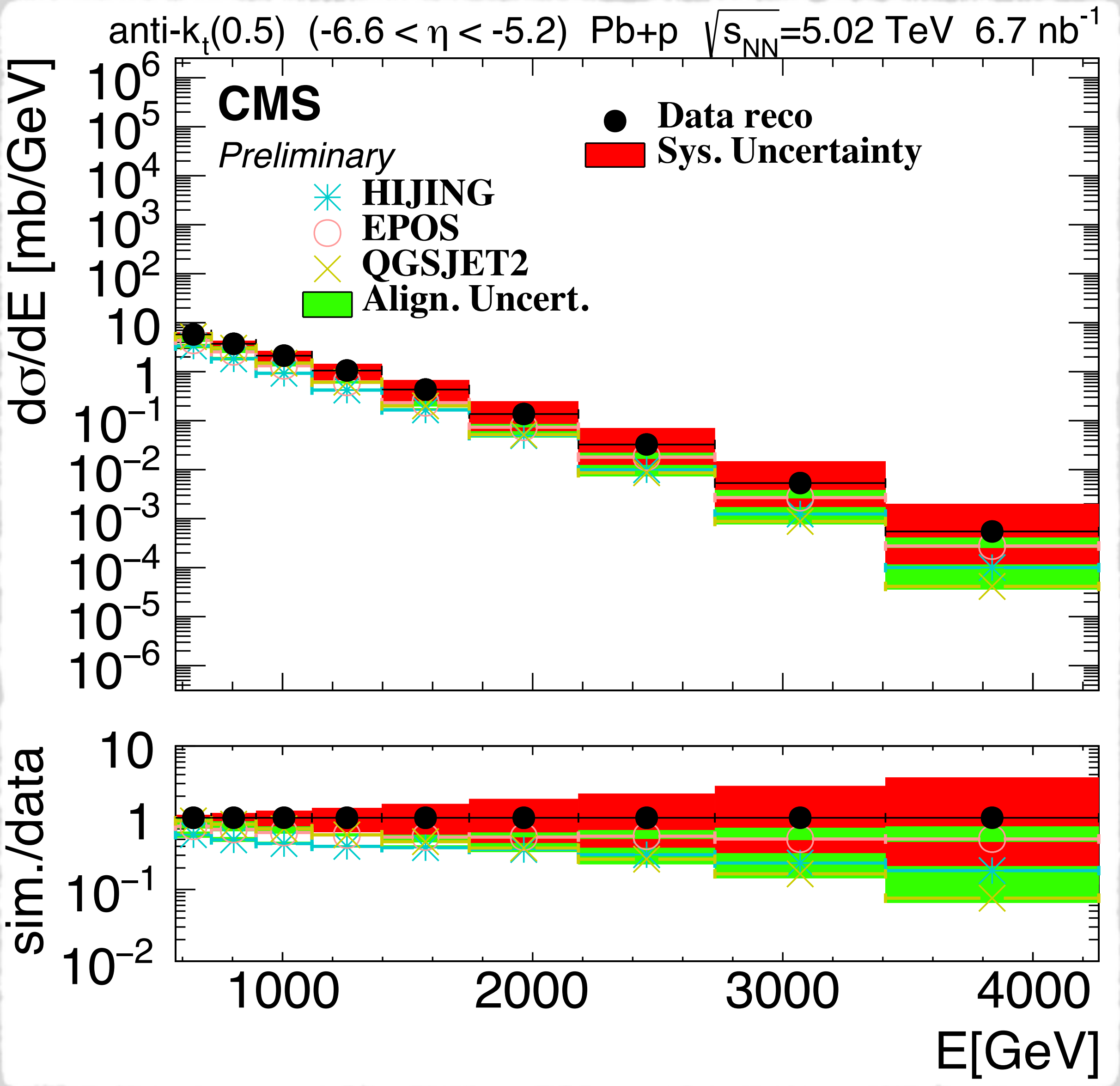

Ratio of jet spectra (unfolded)

Public
CMS-FSQ-17-001

HIJING
shape ✓
norm ✗

EPOS-LHC
low E ✓
high E ✗

QSGJET
low E ✓
shape ✓

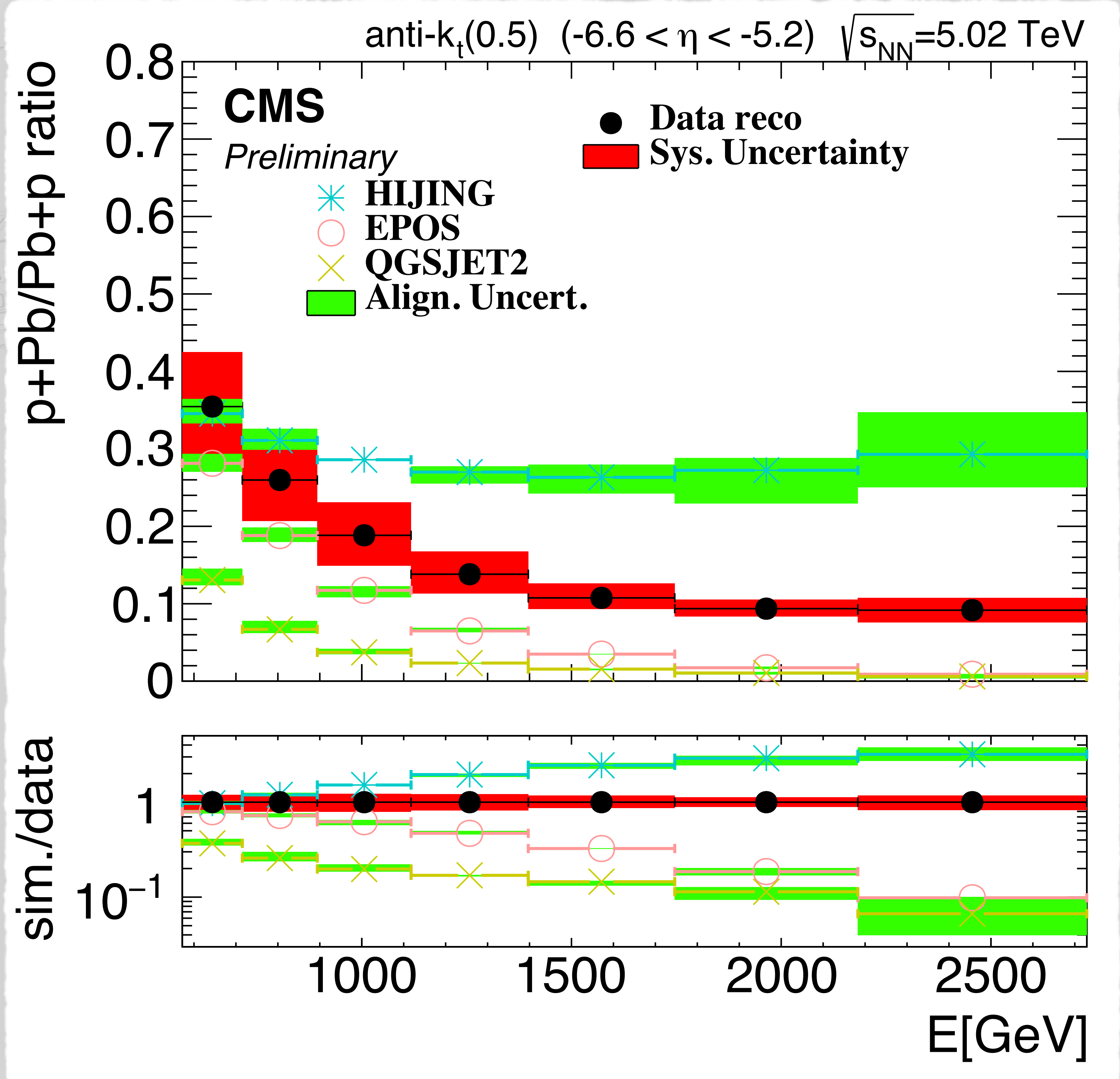

inclusive spectra

Measurement of the inclusive energy spectrum in the very forward direction in proton-proton collisions at $\sqrt{s}$ = 13 TeV

Very forward production

JHEP **08** (2017) 046
CMS-FSQ-16-002

- The production of particles at large rapidities (typically $|\eta| > 5$) are used to investigate:
  1. multiparton interactions (MPI);
  2. initial- and final-state radiation;
  3. fragmentation of beam remnants; and
  4. diffraction.

Very forward production

JHEP **08** (2017) 046
CMS-FSQ-16-002

- The production of particles at large rapidities (typically $|\eta| > 5$) are used to investigate:

  1. multiparton interactions (MPI);
  2. initial- and final-state radiation;
  3. fragmentation of beam remnants; and
  4. diffraction.

a.k.a. **underlying events**

Very forward production

JHEP **08** (2017) 046
CMS-FSQ-16-002

- The production of particles at large rapidities (typically |η| > 5) are used to investigate:
  1. multiparton interactions (MPI);
  2. initial- and final-state radiation;
  3. fragmentation of beam remnants; and
  4. diffraction.

a.k.a.
underlying events

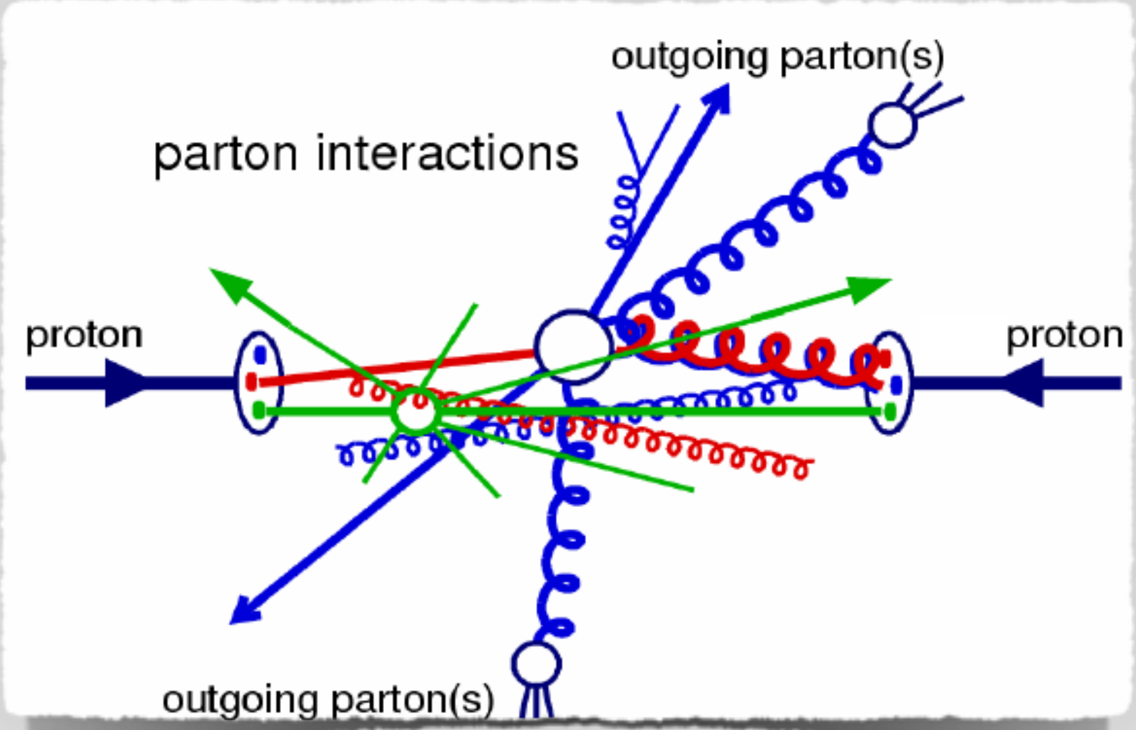

Very forward production

JHEP **08** (2017) 046
CMS-FSQ-16-002

- The production of particles at large rapidities (typically $|\eta| > 5$) are used to investigate:

  1. **multiparton interactions (MPI);**
  2. initial- and final-state radiation;
  3. fragmentation of beam remnants; and
  4. diffraction.

a.k.a.
underlying events

- CASTOR data at 13 TeV is used in this analysis given its **sensitivity** to MPI;
  - Few reports on proton-proton collisions at 0.9, 2.76, 7 and 8 TeV.
  - This report focus on **electrons**, **photons** (π^0 decays), **hadrons** ($\pi^{\pm}$).

Event selection

JHEP **08** (2017) 046
CMS-FSQ-16-002

- Particles are selected in **both** sides of the gap with invariant masses M_X and M_Y;
  - The **momentum loss of the proton** is variable used to select the events, which is a common variable in diffractive physics:

$$\xi_{X,Y} = \frac{M^2_{X,Y}}{s}$$

$$\xi = \max(\xi_X, \xi_Y)$$

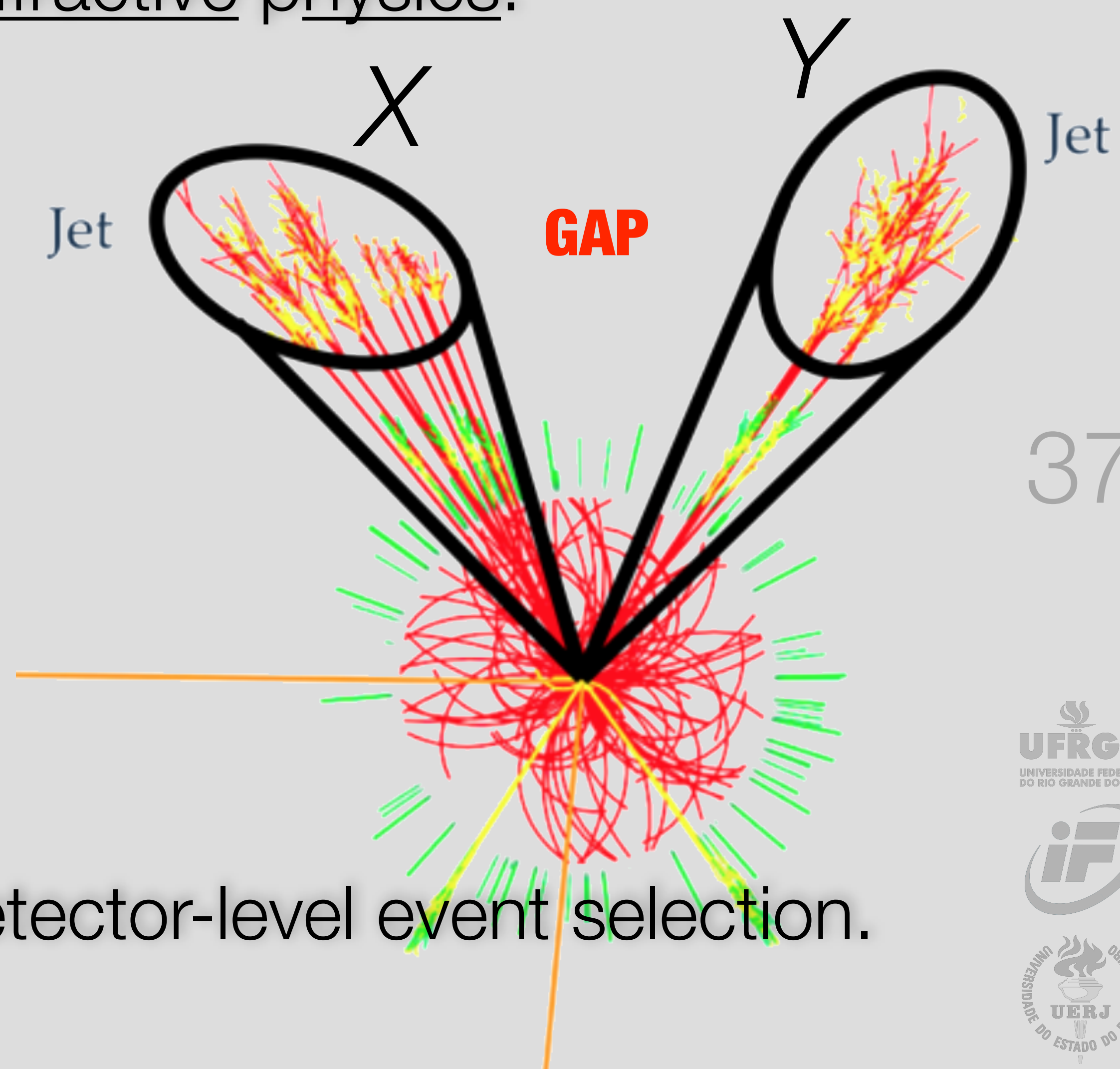

- Events with $\xi > 10^{-6}$ are selected:
  - 97.3% eff. and 99.5% purity w.r.t. the detector-level event selection.

Energy spectra (unfolded)

JHEP **08** (2017) 046
CMS-FSQ-16-002

- Data is compared with Monte Carlo models at particle-level spectra;
- **Best** results with EPOC and QGSJET; PYTHIA tunes <u>overestimate</u> the data.

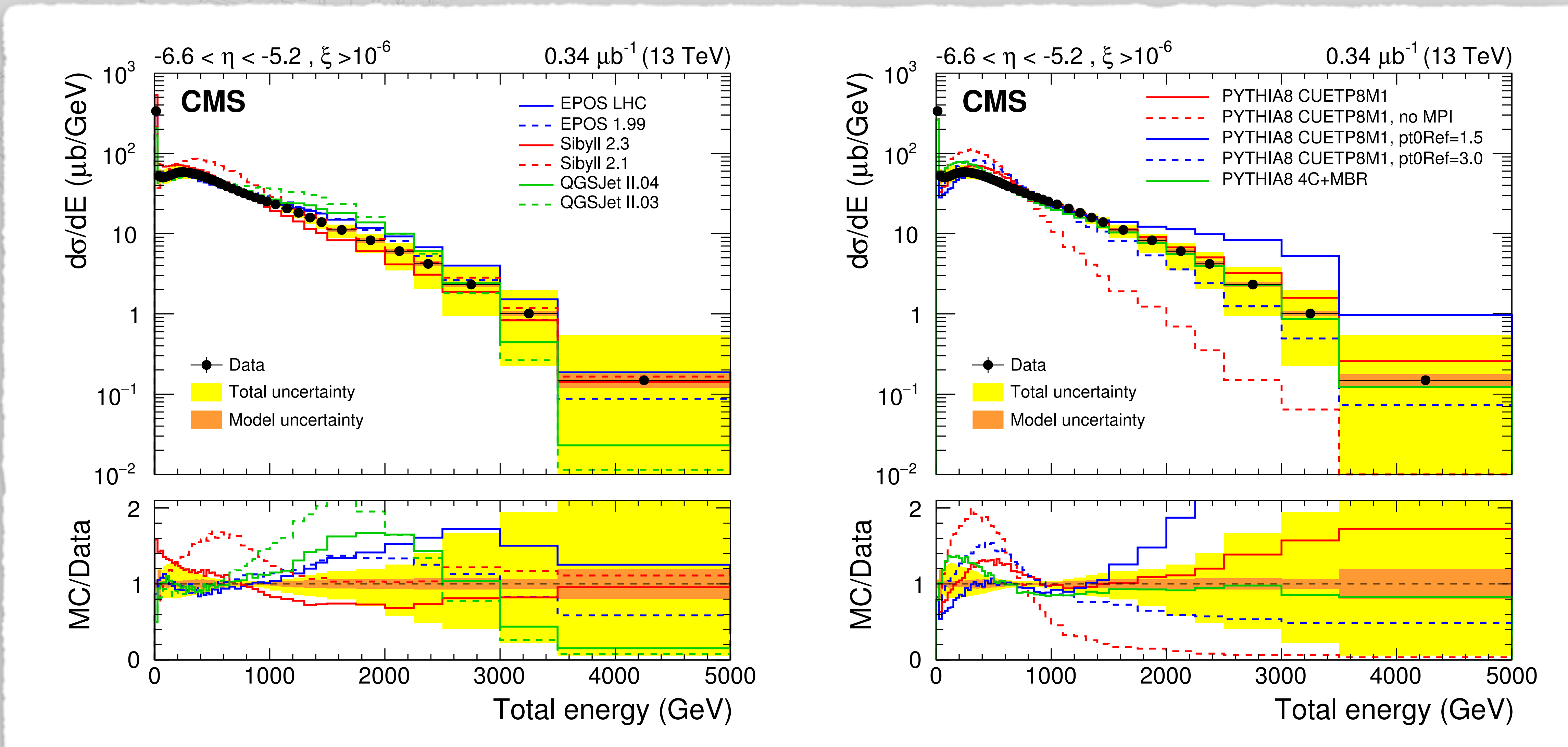

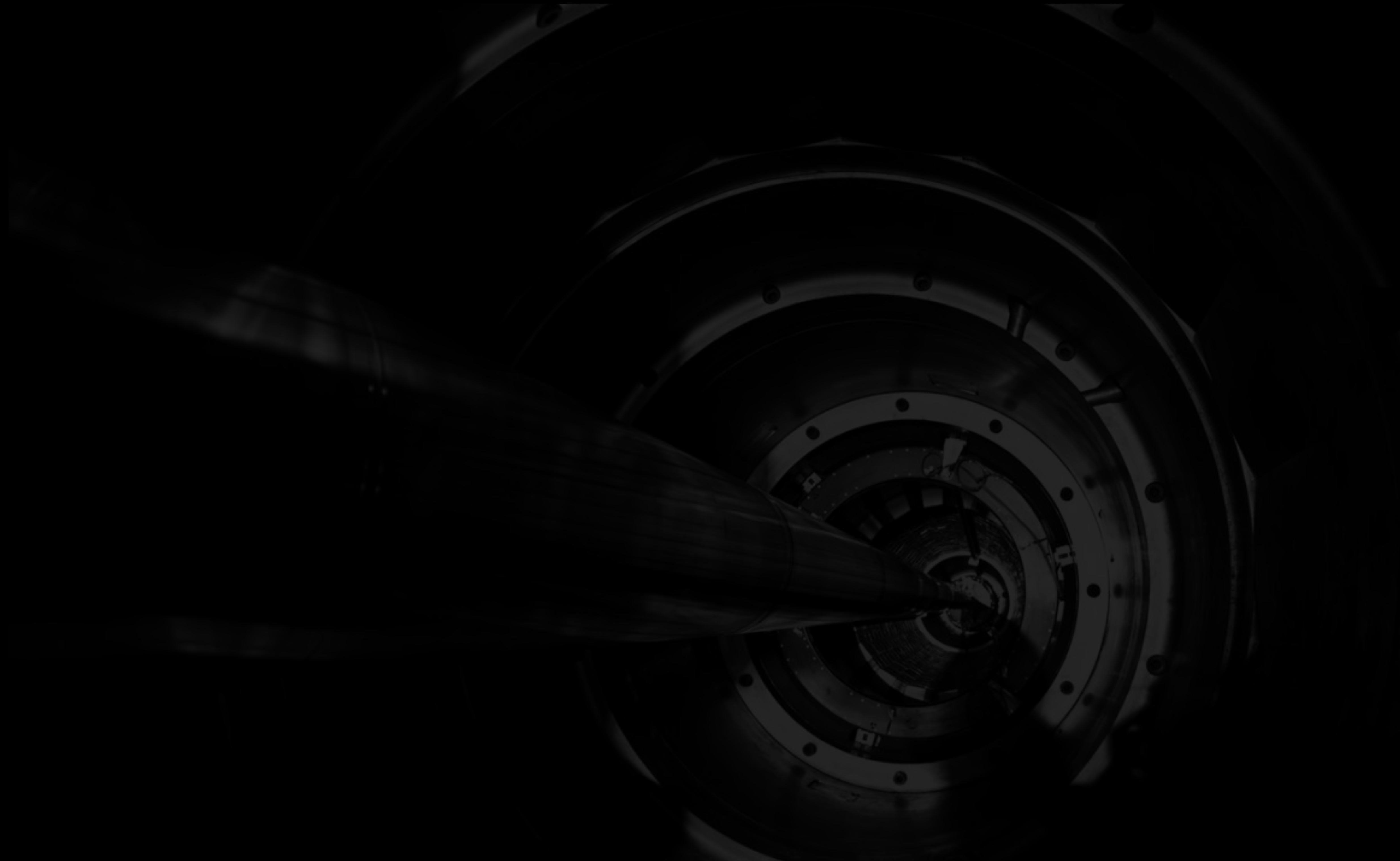

Dijets with leading proton

Measurement of dijet production with a leading proton in proton-proton collisions at 8 TeV with the CMS and TOTEM detectors at the LHC

Proton detection

Public CMS-FSQ-12-033

- Both CMS and TOTEM detectors are employed to detect a **scattered proton** from a diffractive event;

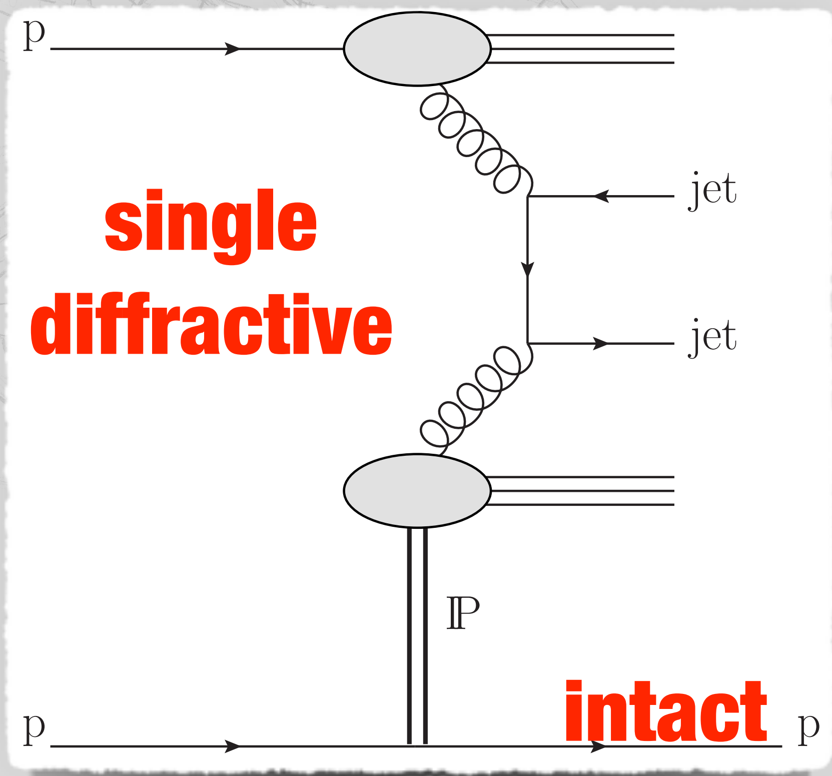

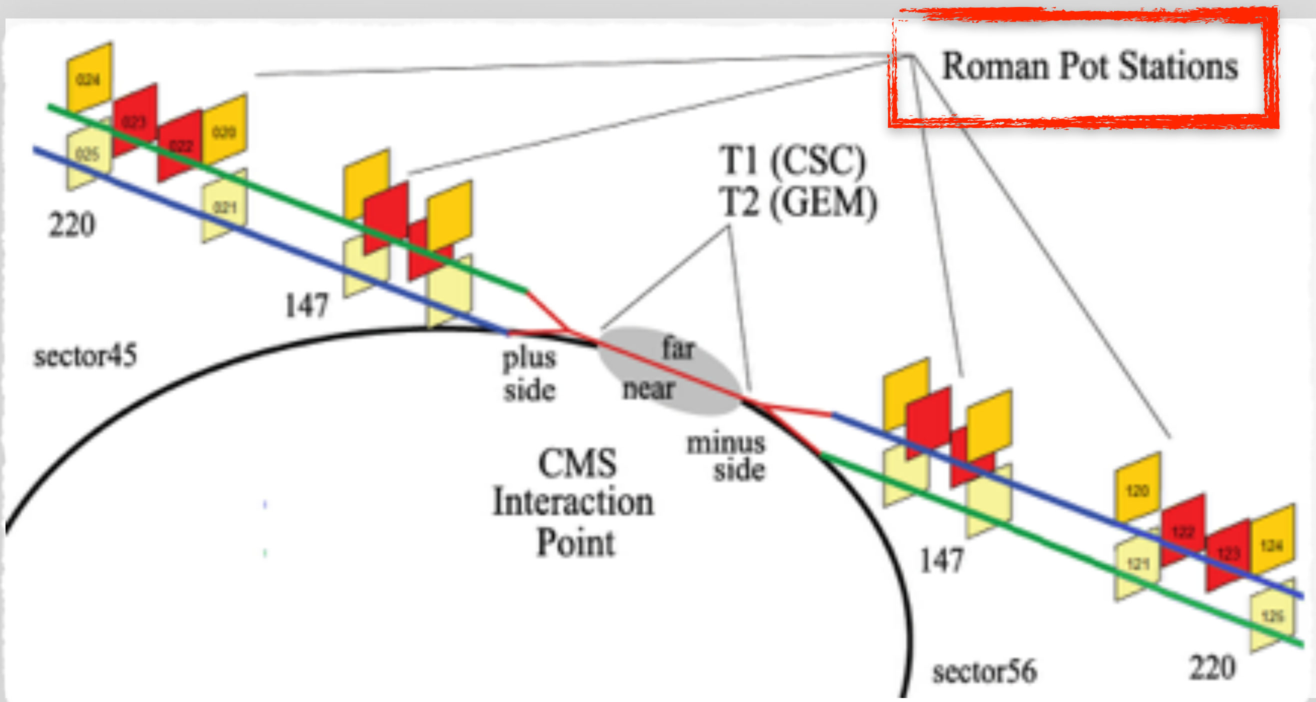

- In a diffractive interaction, the intact proton is scattered at **small angles**;
  - TOTEM **Roman Pots** are used to collect this information;
  - TOTEM acceptance **increases** the CMS pseudorapidity coverage.

Event selection

Public
CMS-FSQ-12-033

- The usual variables for diffractive interactions related the momentum loss by the proton:

$$t = (p_i - p_f)^2$$

$$\xi = 1 - \frac{|p_f|}{|p_i|}$$

CMS-only information →

$$\xi^{\pm}_{\mathrm{CMS}} = \frac{\sum(E^i \pm p_z^i)}{\sqrt{s}}$$

- An amount of **37.5/nb** of data is analyzed to measure the **single-diffractive cross section** in terms of *t* and *ξ*;

$$p_T(jj) > 40\ \mathrm{GeV}, \quad |\eta(jj)| < 4.4$$

$$0.03 < |t| < 1.0\ \mathrm{GeV}^2, \quad 0 < \xi < 0.1$$

Cross section (unfolded)

Public
CMS-FSQ-12-033

- The cross section are determined as

$$\frac{d\sigma_{jj}}{dt} = \mathcal{U}\left\{\frac{N^i_{jj}}{\mathcal{L}A^i\Delta t^i}\right\} \qquad \frac{d\sigma_{jj}}{d\xi} = \mathcal{U}\left\{\frac{N^i_{jj}}{\mathcal{L}A^i\Delta \xi^i}\right\}$$

- N_{jj}: #dijets in *i*-th bin;
- $\mathcal{L}$: luminosity
- A: acceptance
- Δt, Δξ: bin widths
- $\mathcal{U}$: unfolding corrections based on Monte Carlo studies.

MC comparison:

POMWIG

PYTHIA8 4C

PYTHIA8 CUETP8M1

PYTHIA8 Dynamic Gap

Gap survival probability:

$\langle S^2 \rangle$ = 7.4%

(from Data/MC ratio)

Results

Public
CMS-FSQ-12-033

- The cross section measurement by CMS:

$$\sigma = 21.7 \pm 0.9\ (\text{stat.})\ {}^{+3.0}_{-3.3}\ (\text{syst.})\ \pm 0.9\ (\text{lumi.})\ \text{nb}$$

- In agreement with PYTHIA8 Dynamic Gap model: **σ = 23.7 nb**.

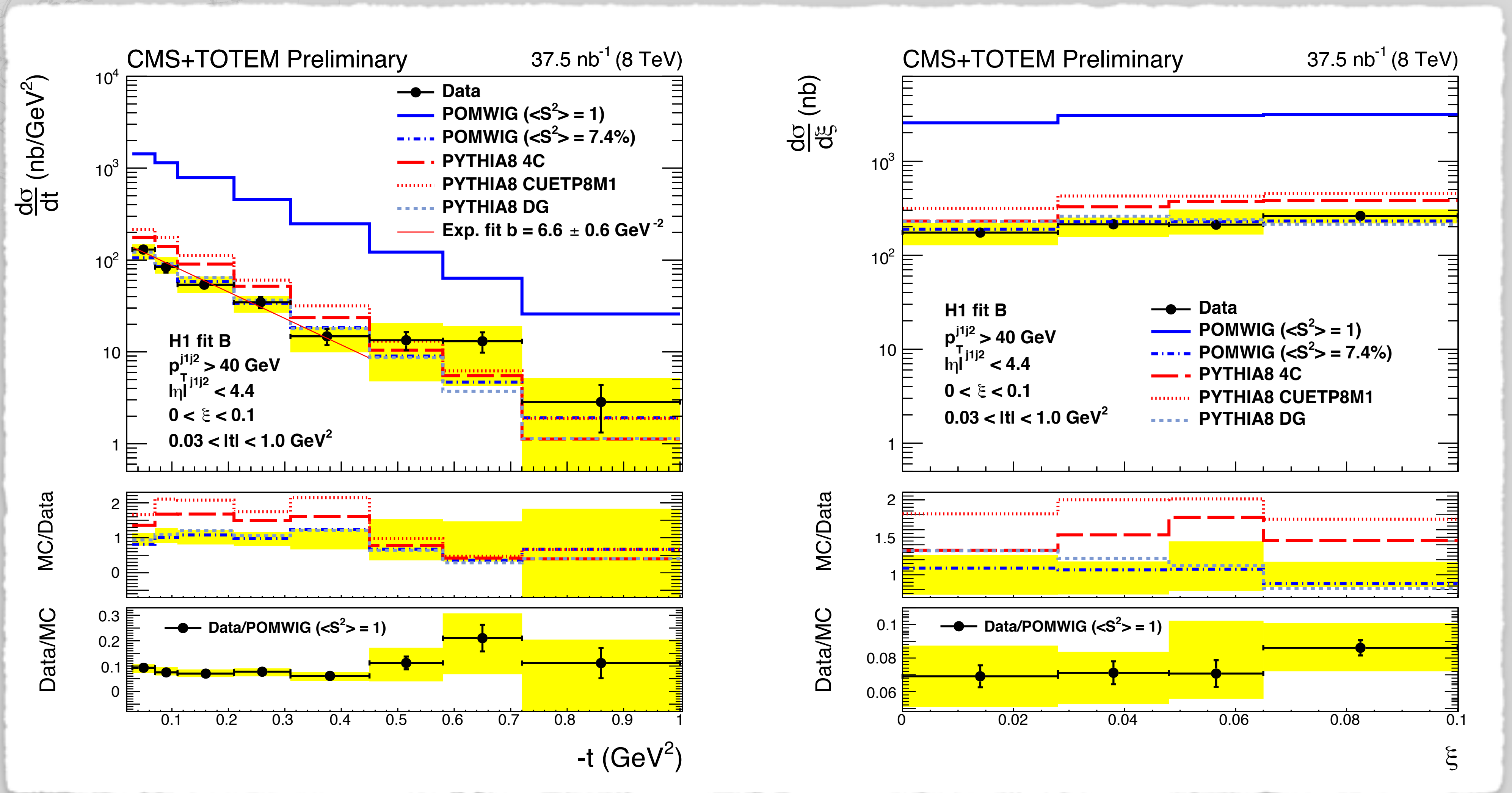

Ratio to inclusive jets

Public
CMS-FSQ-12-033

$$R = \frac{(\sigma_{jj}^{pX}/\Delta\xi)}{\sigma_{jj}} = 0.025 \pm 0.001\ (\text{stat.}) \pm 0.003\ (\text{syst.})$$

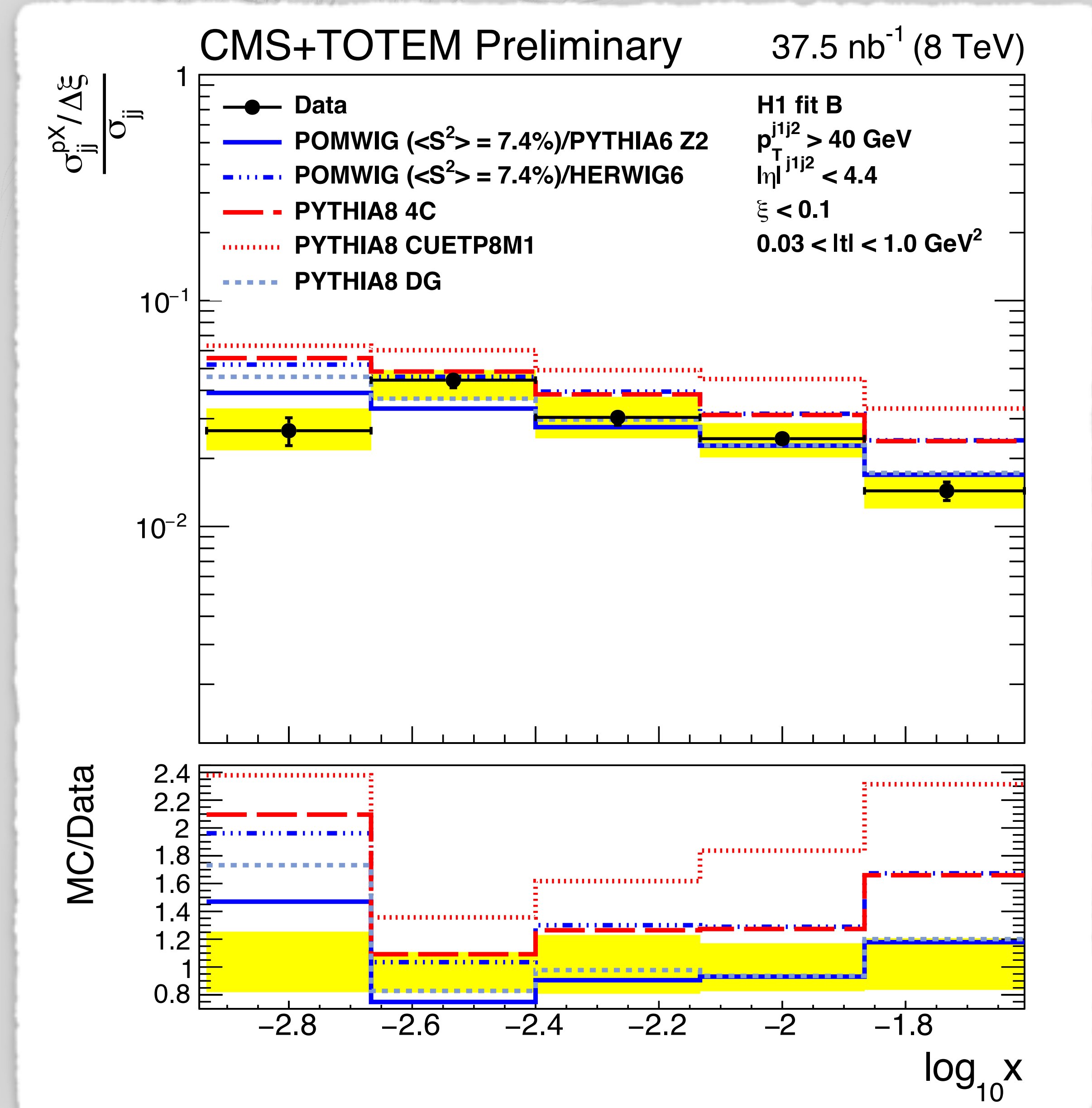

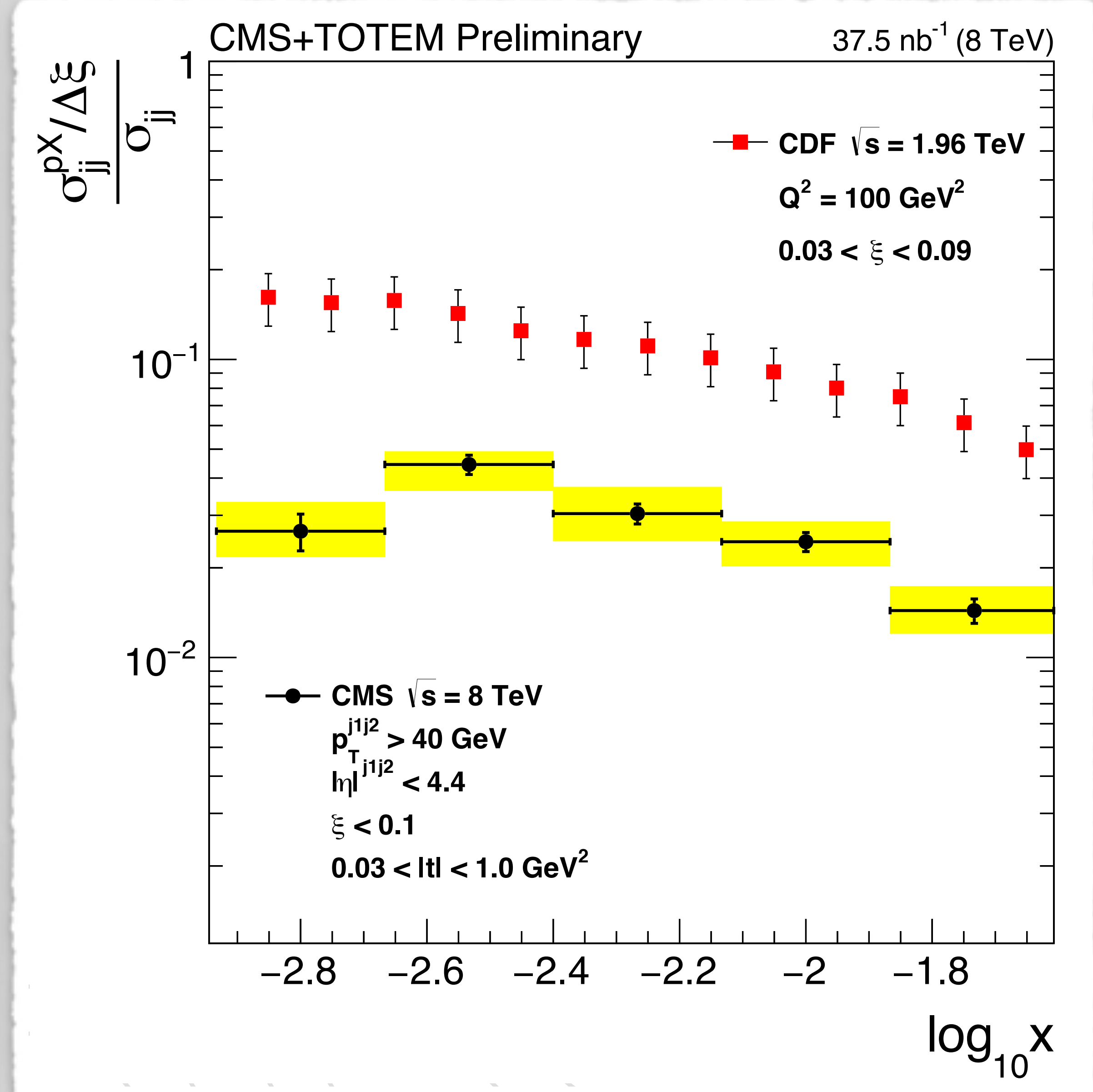

2-photon dilepton production

Observation of proton-tagged, central (semi)exclusive production of high-mass lepton pairs in pp collisions at 13 TeV with the CMS-TOTEM precision proton spectrometer

Experimental setup of PPS

JHEP **07** (2018) 153
CMS-PPS-17-001

- The PPS detector makes use of TOTEM Roman Pots (RP) to allocate **tracking** and **timing** detectors (sectors 45 and 56):

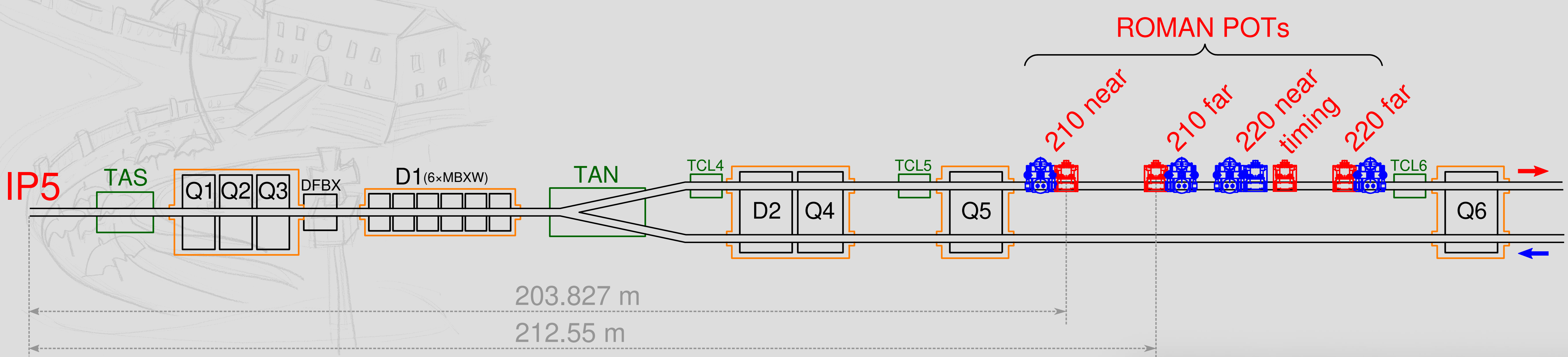

- Scattered protons with **84—97%** of the incoming beam momentum are detected;
- 2016 configuration: tracking detectors are silicon sensors with 512 strips.
  - In 2017, PPS moved to **3D pixel detectors**.

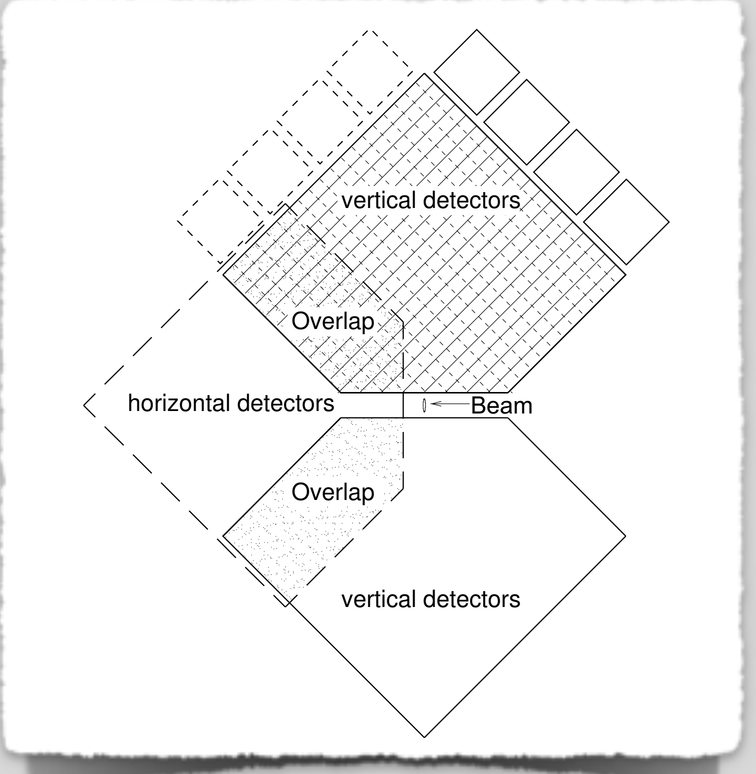

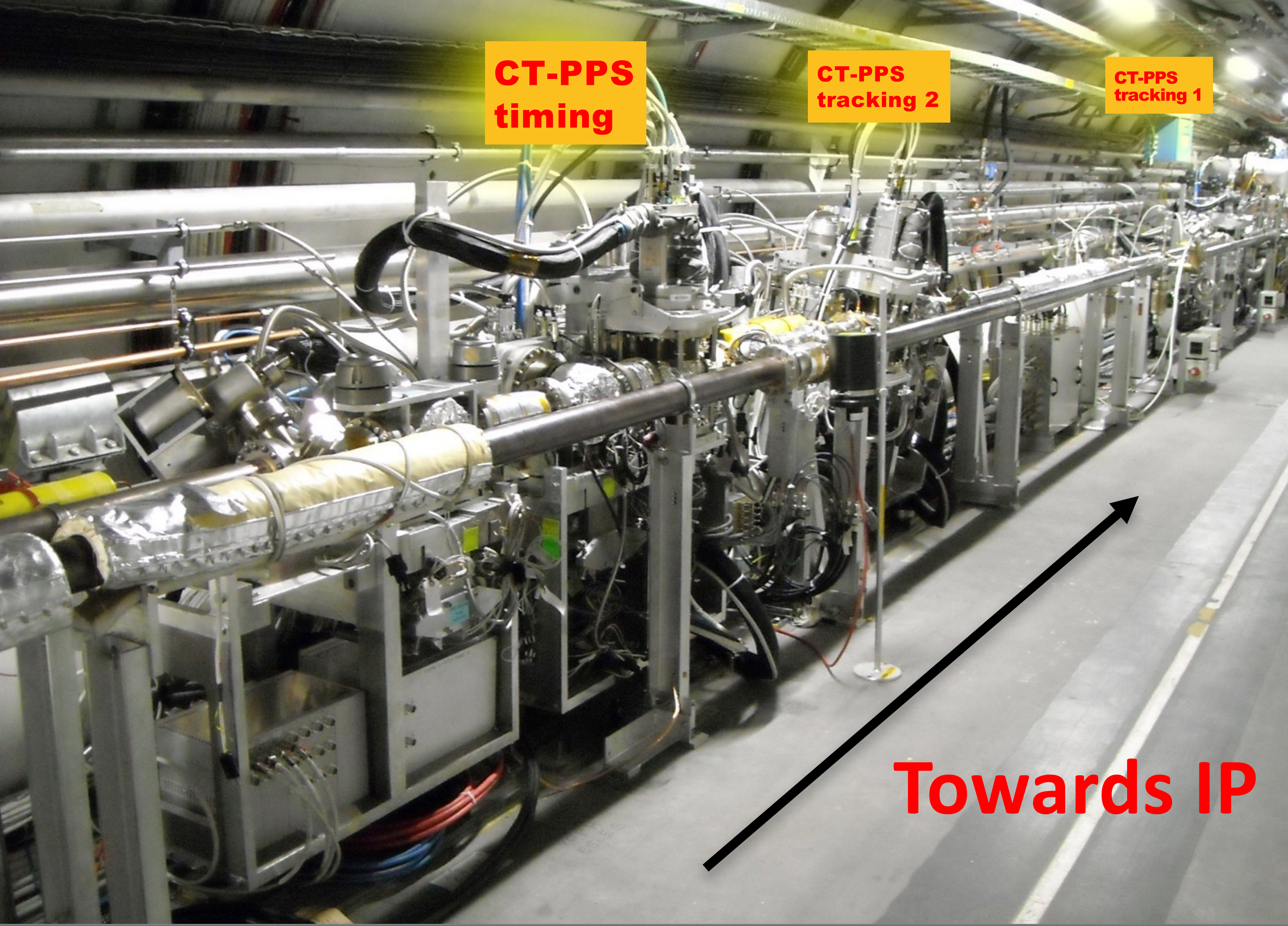
CT-PPS
timing
CT-PPS
tracking 2
CT-PPS
tracking 1
Towards IP

Two-photon production

JHEP **07** (2018) 153
CMS-PPS-17-001

- Apart of diffractive production, the two-photon interaction is also an elastic collision with intact protons scattered at **small angles**;

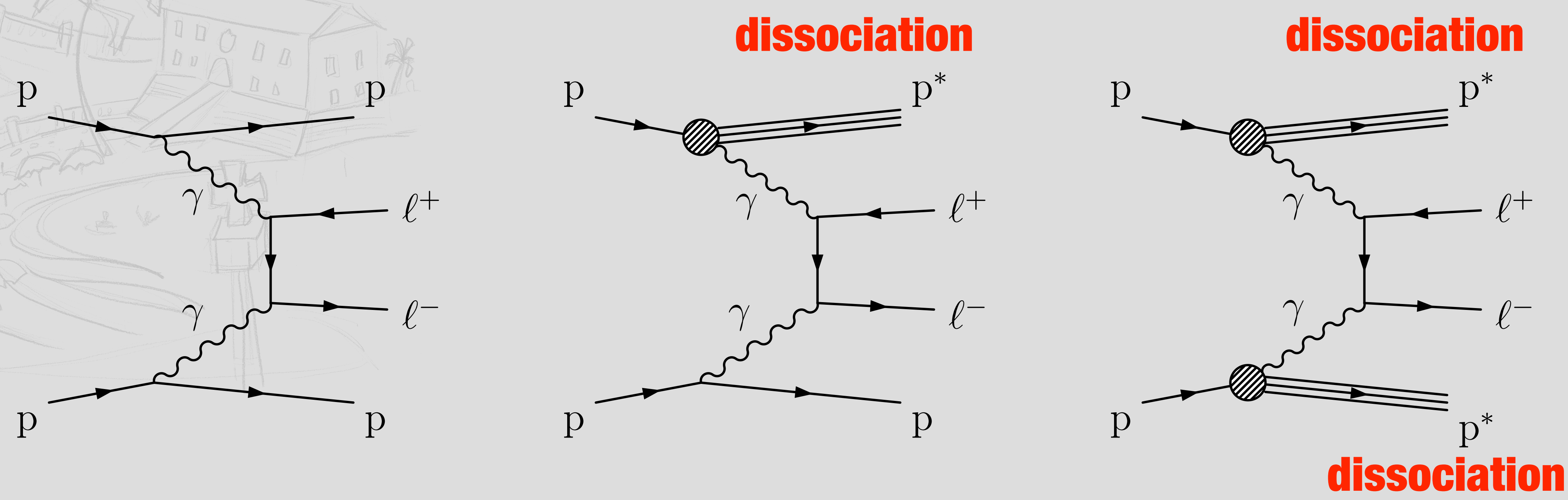

- The Precision Proton Spectrometer is meant to measure the **forward protons** of the elastic interaction at **a high-luminosity regime**;
  - Acceptance for protons detected in both arms start at ***M*(ll) ≳ 400 GeV**;
  - Adding semi-exclusive events can increase data sample.

Event selection

JHEP **07** (2018) 153
CMS-PPS-17-001

- The analysis considers **9.4/fb** of 2016 data to search for (semi-)exclusive dilepton production;

- The strategy follows the approaches employed in previous CMS analyses;

  1. Leptons are selected with p_T > 50 GeV with opposite charge;
  2. **No tracks** from the vertice given a veto distance;
  3. Consistent back-to-back leptons based on **acoplanarity**;
  4. Dileptons with invariant mass **above 110 GeV**.

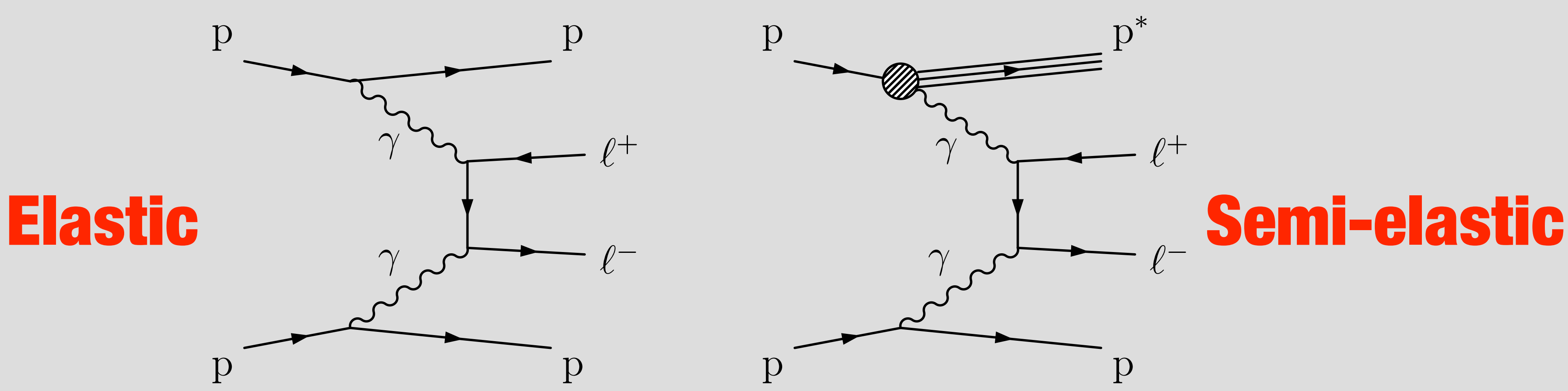

Event selection

JHEP **07** (2018) 153
CMS-PPS-17-001

- The analysis considers **9.4/fb** of 2016 data to search for (semi-)exclusive dilepton production;

- The strategy follows the approaches employed in previous CMS analyses;

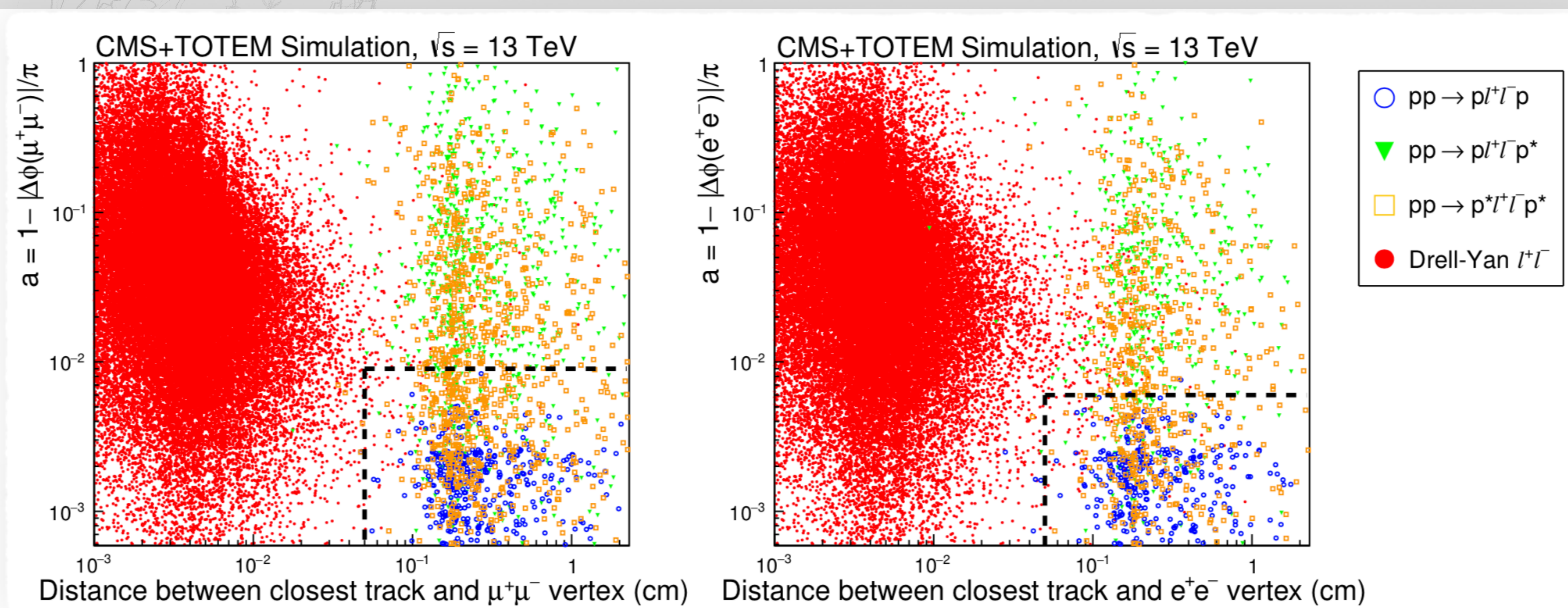

Central detector

JHEP **07** (2018) 153
CMS-PPS-17-001

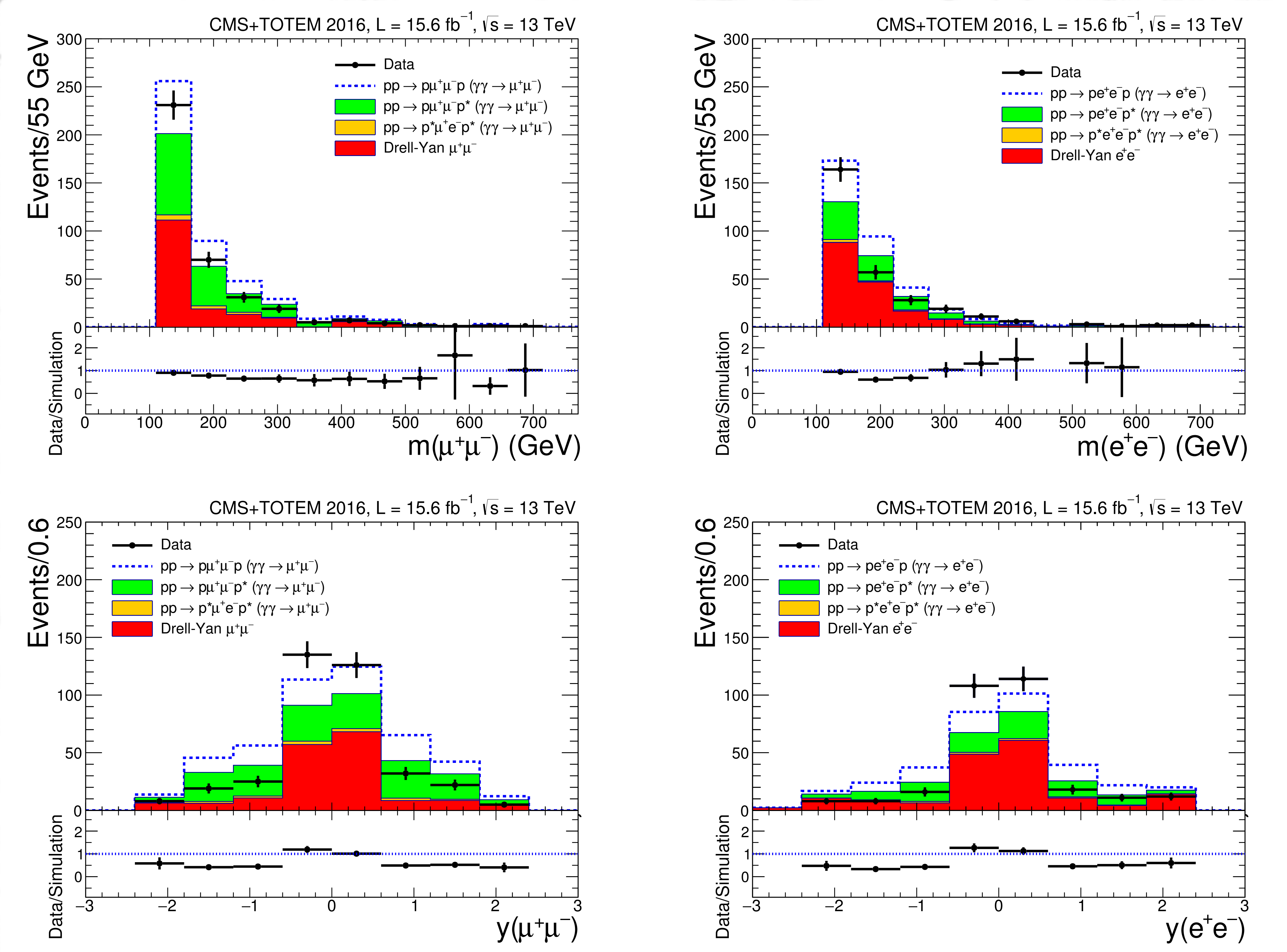

51

Matching

JHEP **07** (2018) 153
CMS-PPS-17-001

- Signal events in the central detector are **directly related** to the scattered protons measured with PPS;

- Proton momentum loss is **matched** with that of the dileptons:

$$\xi(\ell^+\ell^-) = \frac{1}{\sqrt{s}}\left[p_{\mathrm{T}}(\ell^+)\mathrm{e}^{\pm\eta(\ell^+)} + p_{\mathrm{T}}(\ell^-)\mathrm{e}^{\pm\eta(\ell^-)}\right]$$

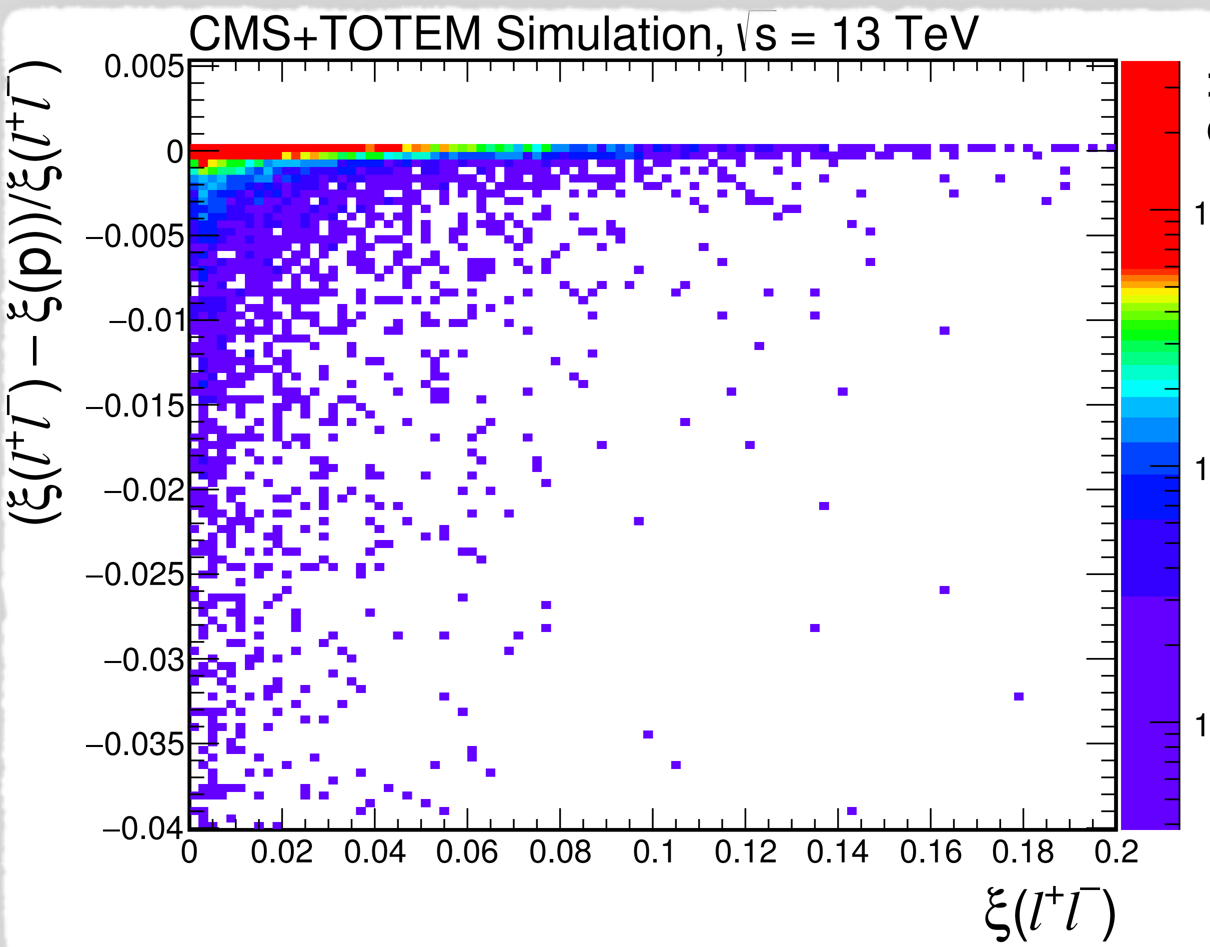

- Different acceptances depend on **stations** and **beamline positions**:
  - sector 45, RP 210N: $\xi > 0.033$,
  - sector 45, RP 210F: $\xi > 0.024$,
  - sector 56, RP 210N: $\xi > 0.042$,
  - sector 56, RP 210F: $\xi > 0.032$.

Results

JHEP **07** (2018) 153
CMS-PPS-17-001

- A total of **12 events** ($\mu^+\mu^-$) and **8 events** (e^+e^-) are observed;
  - Significances are 4.3σ ($\mu^+\mu^-$) and 2.6σ (e^+e^-): **combined >5σ**
  - **Consistent** with MC predictions within acceptance and overall efficiency.

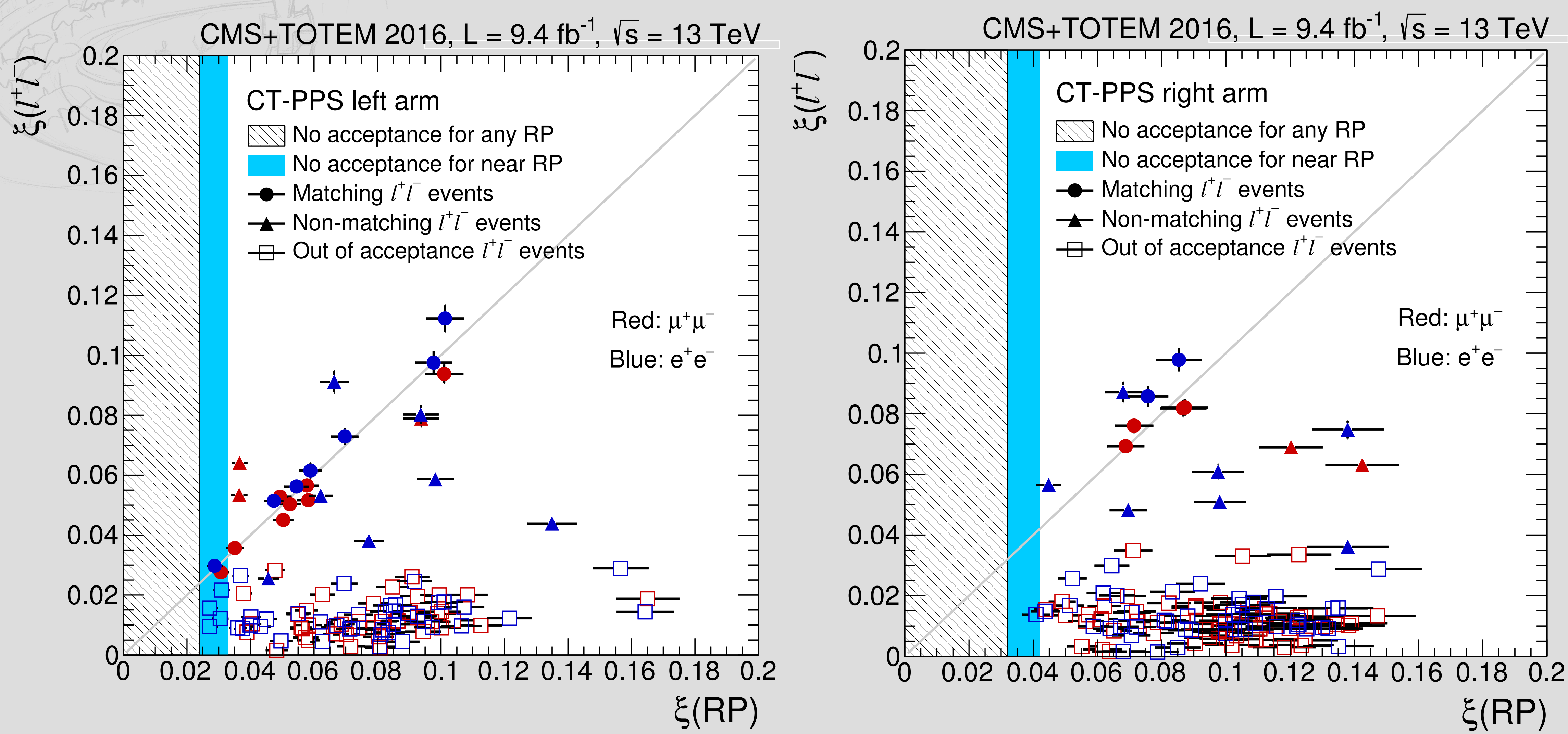

Acceptance

JHEP **07** (2018) 153
CMS-PPS-17-001

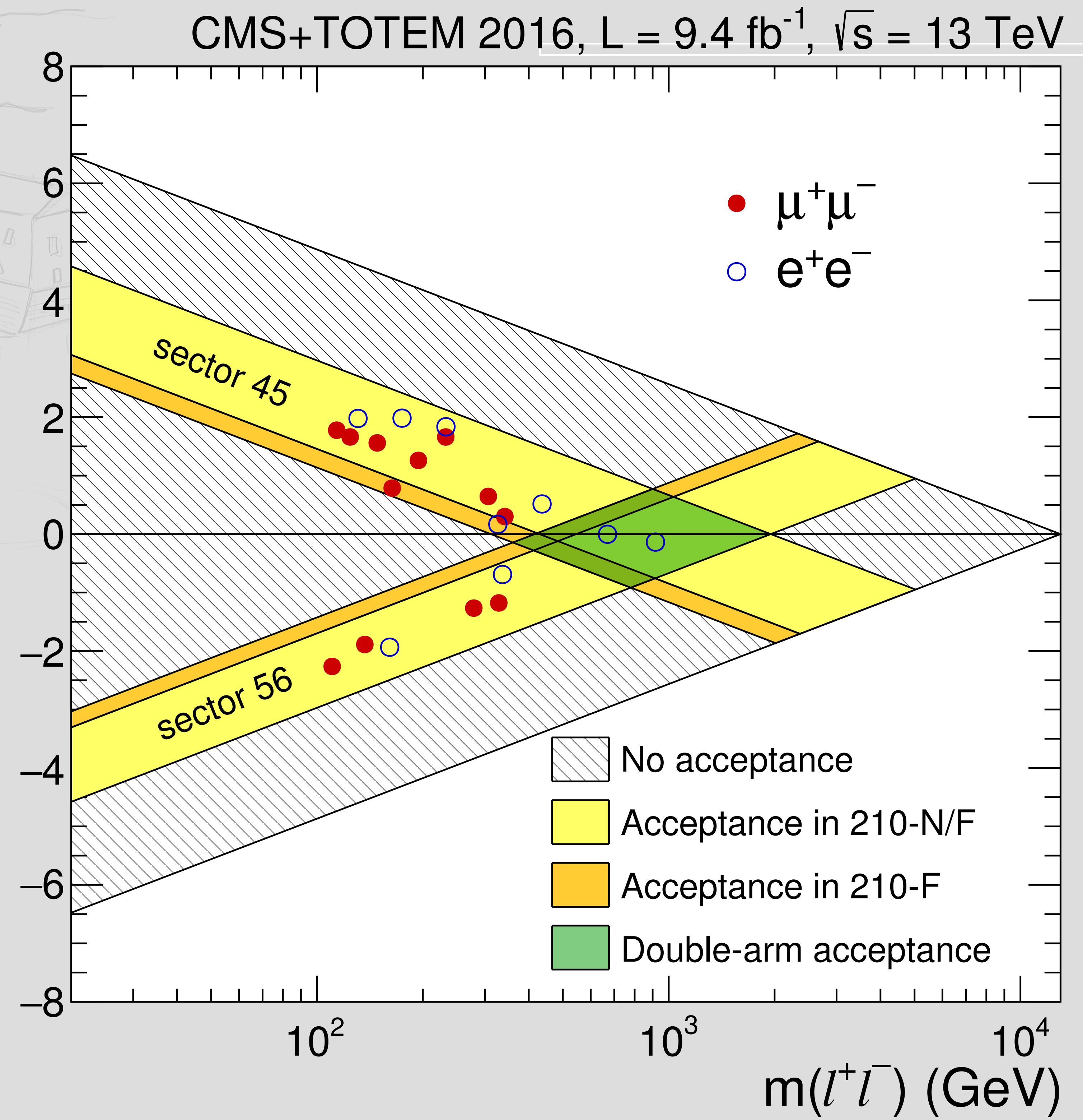

Summary

- The CMS detector has shown its capability for measuring forward tracks with **high efficiency**;
- These reports cover important physics aspects like:
  - Detailed study of **underlying events** at 7 TeV;
  - **Saturations effects** at high-gluon density;
  - **Central diffractive** production of jets; and
  - First results of the new **forward detector PPS**.

- More interesting reports to come in **2018** with additional data from RunII.

Backup slides

Additional information about the analyses

Hadronic Forward

- Both sides of CMS: **HF+** | **HF–**;
- <u>Long</u> and <u>short</u> quartz fibers (~2k ch);
  - Electromagnetic and Hadronic parts
- Specialized to measure:
  1. Elastic/Diffractive xsec;
  2. Forward energy flow;
  3. Jet spectra and correlations.

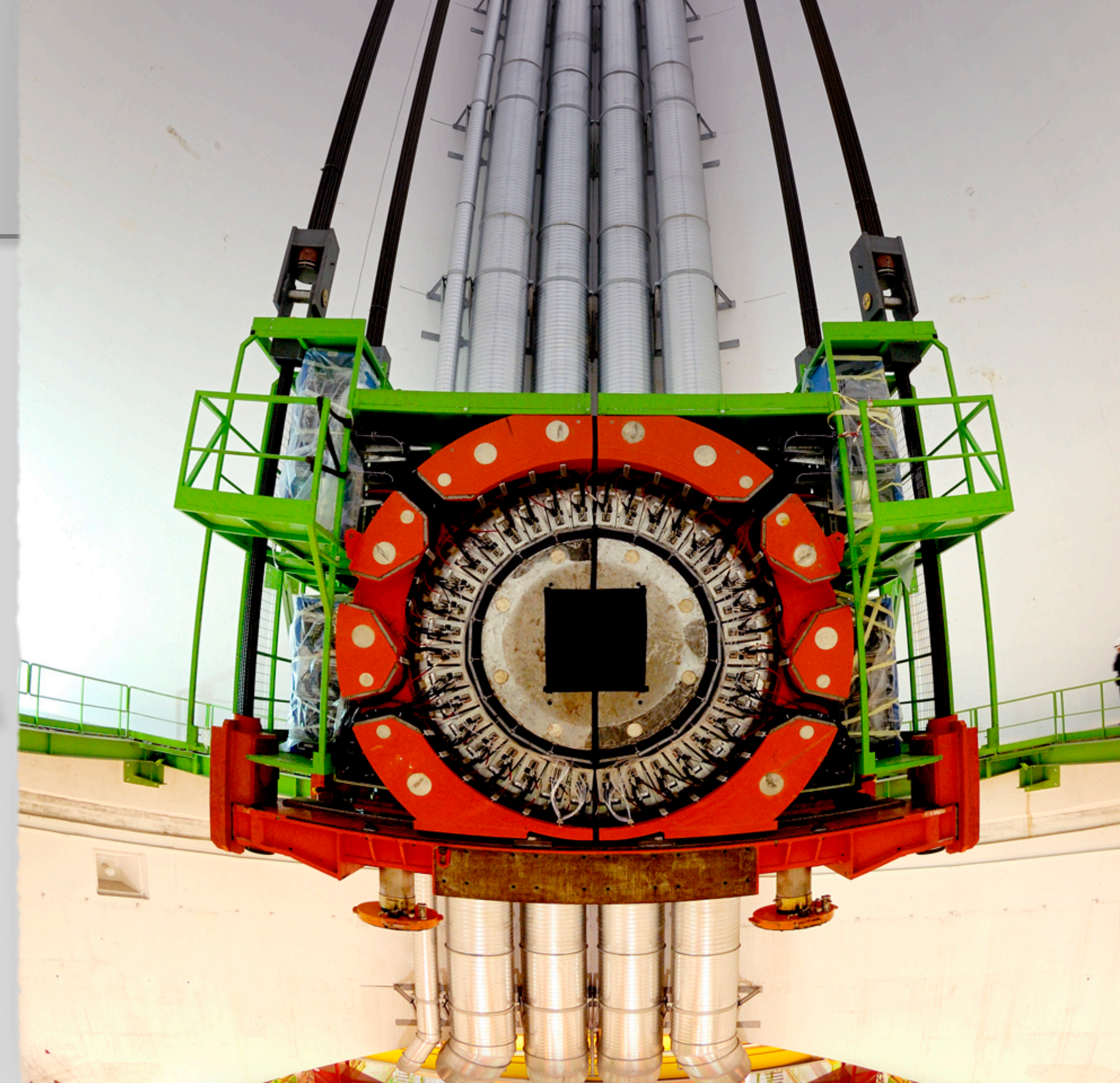

CASTOR

- Tungsten and quartz plates as a sampling calorimeter;
- Only at minus side of CMS;
- No segmentation on η — energy spectra instead of p_T;

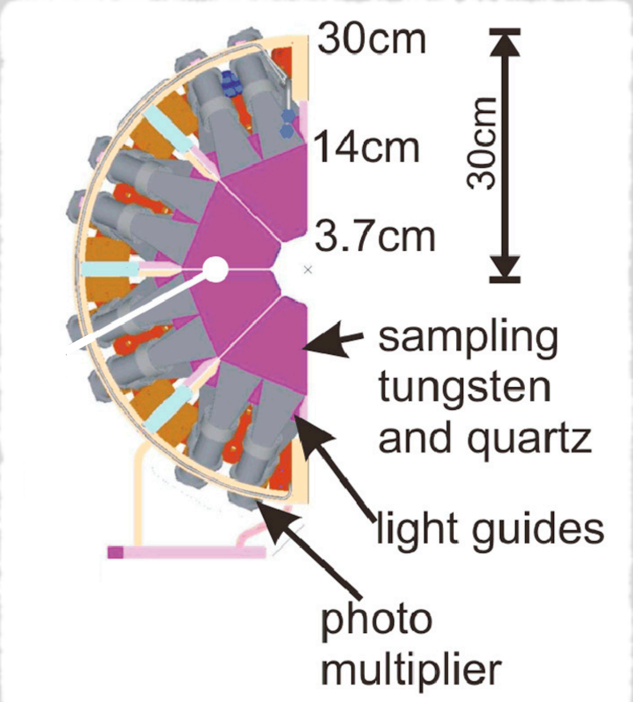

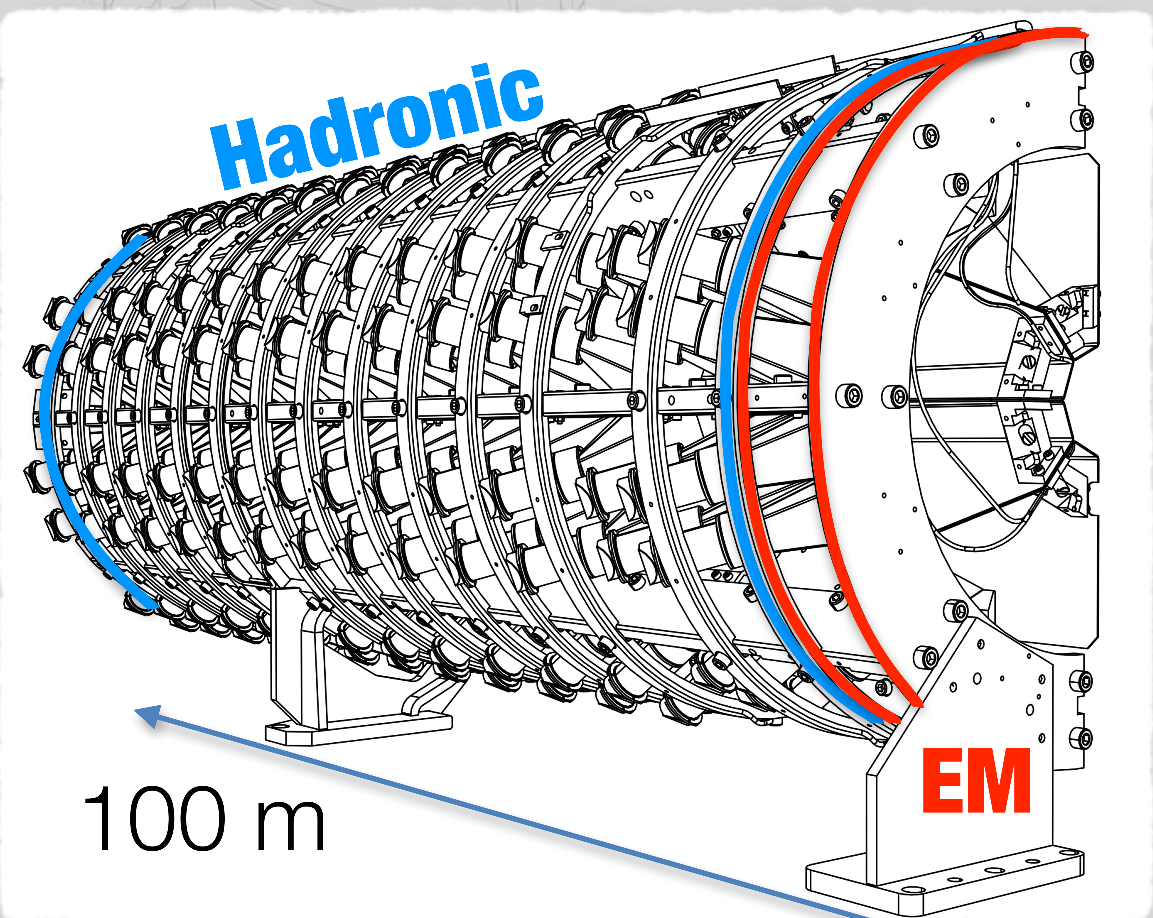

- CASTOR measures:
  1. Inelastic/Diffractive xsec;
  2. Forward energy and UE;
  3. jet spectra.

12x hadronic modules

2x EM modules

Jet-Gap-Jet

Source	40–60 GeV	60–100 GeV	100–200 GeV
Jet energy scale	±5.1	±6.7	±2.1
Tracks quality	±0.3	±1.3	±0.4
Background subtraction	±14.1	±0.9	±1.9
Total systematic	±15.0	±6.9	±2.8
Statistical	±23	±22	±15

Inclusive jets

Source uncertainty	p+Pb		Pb+p		p+Pb/Pb+p	
	600 GeV	2.5 TeV	600 GeV	2.5 TeV	600 GeV	2.5 TeV
Energy scale	+2% −2%	+145% −71%	+6% −6%	+170% −82%	+5% −7%	+57% −9%
Model dependence	+14% −14%	+37% −37%	+13% −13%	+46% −46%	+24% −24%	+48% −48%
Alignment	+3% −3%	+24% −24%	+3% −6%	+49% −24%	+10% −6%	+4% −6%
Jet indentification	+1% −1%	+22% −22%	<1% <1%	<1% <1%	+1% −1%	+21% −21%
Total	+15% −14%	+153% −87%	+15% −16%	+177% −98%	+26% −26%	+77% −54%

Energy deposits in CASTOR

JHEP **08** (2017) 046
CMS-FSQ-16-002

- A total of **0.34/μb** of data is analyzed for CASTOR calibration;
  - Beam halo muons and responde to pions/electrons are employed;
  - The total energy deposited in CASTOR is measured and compared to model predictions.

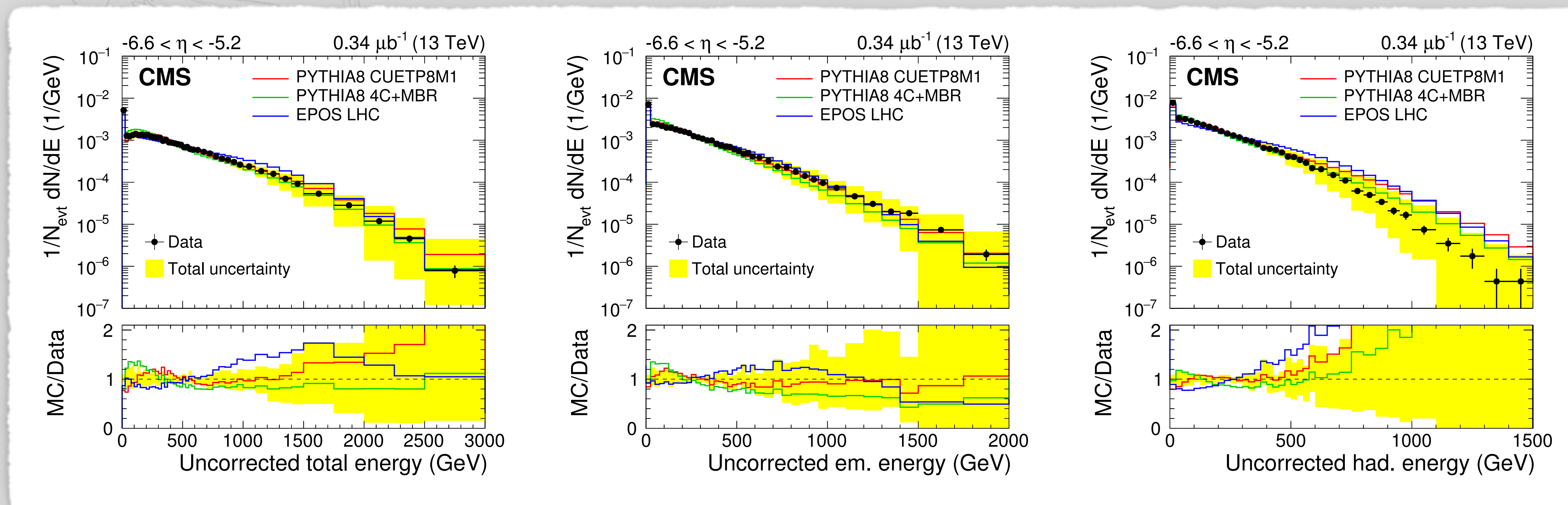

Total **Electromagnetic** **Hadronic**

Inclusive spectra

	Total		Electromagnetic		Hadronic	
	300 GeV	3000 GeV	300 GeV	1200 GeV	300 GeV	2000 GeV
Energy Scale	$^{+17\,\%}_{-14\,\%}$	$^{+94\,\%}_{-77\,\%}$	$^{+5.9\,\%}_{-2.1\,\%}$	$^{+93\,\%}_{-65\,\%}$	$^{+11\,\%}_{-10\,\%}$	$^{+169\,\%}_{-80\,\%}$
Unfolding	±5.8%	±6.4%	±5.2%	±4.1%	±6.9%	±17%
Event selection	±0.5%	<0.01%	±0.14%	<0.01%	±0.06%	<0.01%
Luminosity	±2.6%					
Statistical	±1.2%	±4.3%	±1.5%	±5.9%	±1.0%	±4.2%

Dijets with tagged proton

Uncertainty source	$\Delta\sigma/\sigma$
Trigger efficiency	± 2 %
Calorimeter energy scale	+1/-2 %
Jet energy scale and resolution	+9/-8 %
Background	± 2 %
Resolution	± 2 %
Horizontal dispersion	+9/-12 %
Acceptance and unfolding	± 2 %
Unfolding bias	± 3 %
Total	+14/-15 %

Alignment

JHEP **07** (2018) 153
CMS-PPS-17-001

- It is required to determine the **position** of:

    1. the sensors inside the Roman Pots,

    2. the relative position of the RPs; and

    3. overall PPS position.

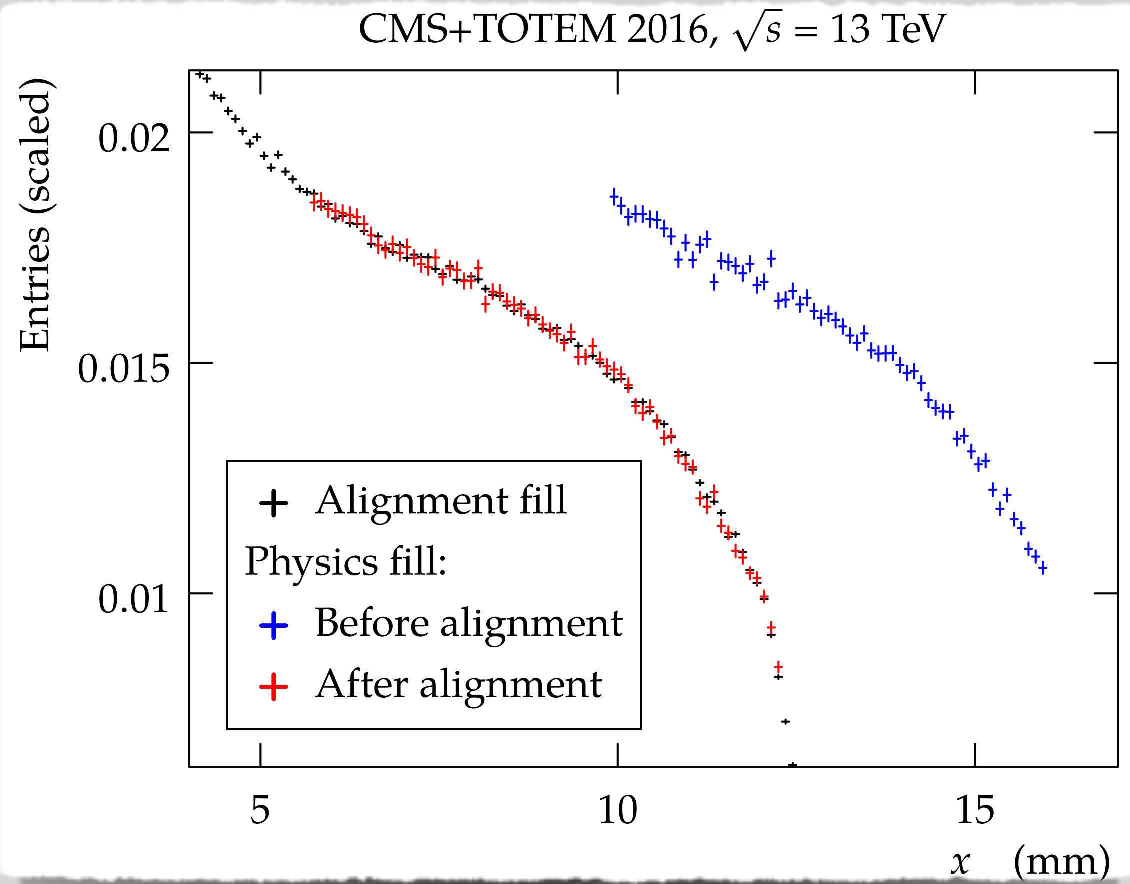

- Alignment fill is used to set the position of the RPs w.r.t. the LHC collimators;

- Physics fills are needed to position of PPS for each fill.

    – The **horizontal alignment** is based on the kinematic distribution of scattered protons in all fill.

Proton reconstruction

JHEP **07** (2018) 153
CMS-PPS-17-001

- The trajectory of the protons in the RPs is a **straight line** given the absence of magnetic fields;
- Hits are studied in each strips with at least 3 hits at 15σ from the beam line;

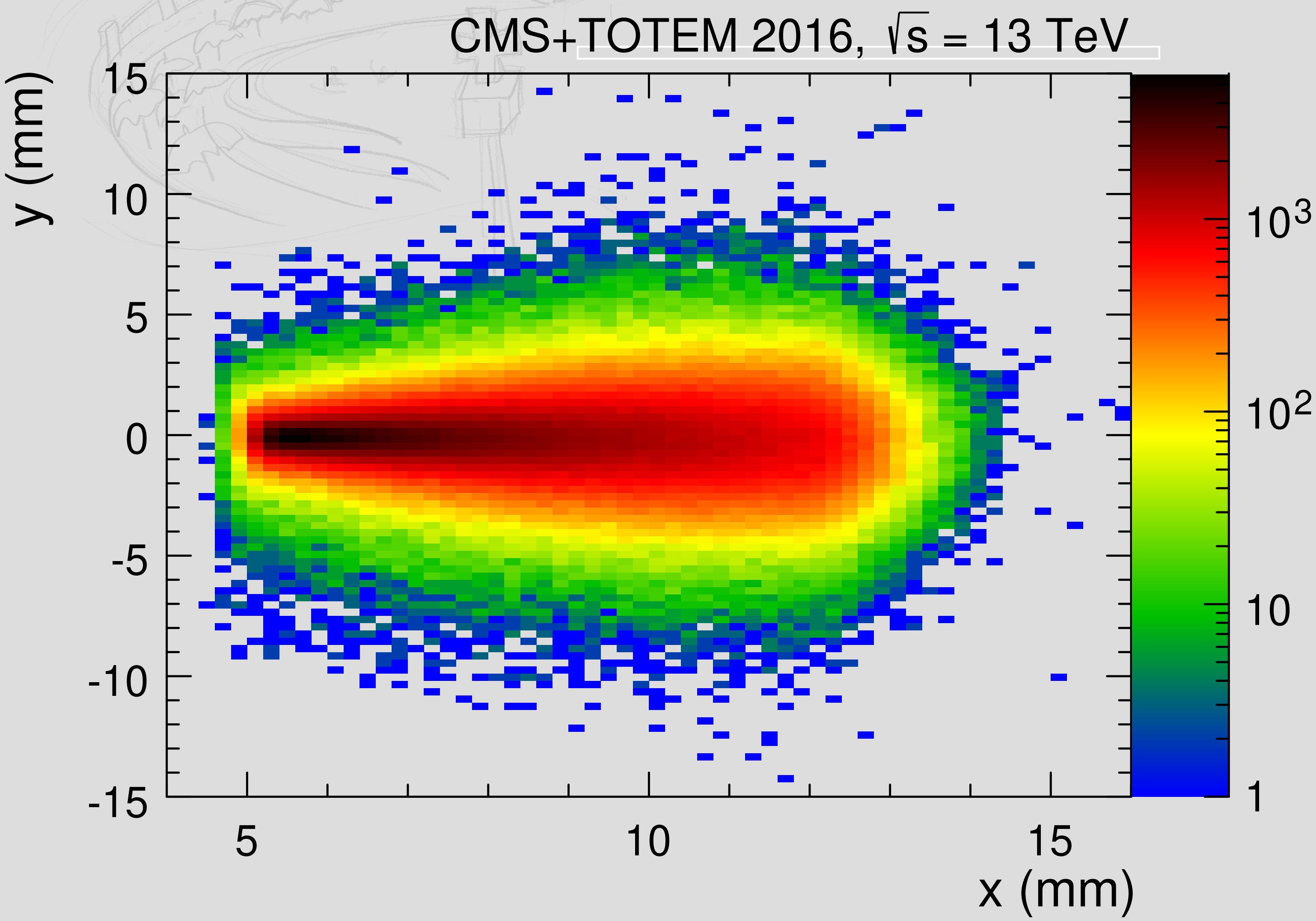

- Inefficiency depends on the pileup and ranges from **15%** to **40%** in 2016 data.

PPS

	$\mu^+\mu^-$		e^+e^-	
Sources of uncertainty	Drell-Yan	Double diss.	Drell-Yan	Double diss.
Statistics of Z sample	5%	5%	4%	4%
$\xi(\ell^+\ell^-)$ reweighting	25%	—	11%	—
Track multiplicity modeling	28%	—	14%	—
Survival probability	—	100%	—	100%
Luminosity	—	2.5%	—	2.5%